



EVOLUTIONARY TRAJECTORIES AND BIOGEOCHEMICAL IMPACTS OF MARINE EUKARYOTIC PHYTOPLANKTON

Miriam E. Katz,¹ Zoe V. Finkel,² Daniel Grzebyk,²
Andrew H. Knoll,³ and Paul G. Falkowski^{1,2}

¹*Department of Geological Sciences, Rutgers University, Piscataway,
New Jersey 08854; email: mimikatz@rci.rutgers.edu*

²*Institute of Marine and Coastal Sciences, Rutgers University, New Brunswick,
New Jersey 08901; email: finkel@imcs.rutgers.edu, grzebyk@imcs.rutgers.edu,
falko@imcs.rutgers.edu*

³*Department of Organismic and Evolutionary Biology, Harvard University,
Cambridge, Massachusetts 02138; email: aknoll@oeb.harvard.edu*

Key Words coccolithophores, diatoms, dinoflagellates, phylogenetic trees,
carbon cycle

■ **Abstract** The evolutionary succession of marine photoautotrophs began with the origin of photosynthesis in the Archean Eon, perhaps as early as 3.8 billion years ago. Since that time, Earth's atmosphere, continents, and oceans have undergone substantial cyclic and secular physical, chemical, and biological changes that selected for different phytoplankton taxa. Early in the history of eukaryotic algae, between 1.6 and 1.2 billion years ago, an evolutionary schism gave rise to "green" (chlorophyll *b*-containing) and "red" (chlorophyll *c*-containing) plastid groups. Members of the "green" plastid line were important constituents of Neoproterozoic and Paleozoic oceans, and, ultimately, one green clade colonized land. By the mid-Mesozoic, the green line had become ecologically less important in the oceans. In its place, three groups of chlorophyll *c*-containing eukaryotes, the dinoflagellates, coccolithophorids, and diatoms, began evolutionary trajectories that have culminated in ecological dominance in the contemporary oceans. Breakup of the supercontinent Pangea, continental shelf flooding, and changes in ocean redox chemistry may all have contributed to this evolutionary transition. At the same time, the evolution of these modern eukaryotic taxa has influenced both the structure of marine food webs and global biogeochemical cycles.

INTRODUCTION

Phytoplankton comprise a diverse, polyphyletic group of single-celled and colonial aquatic photosynthetic organisms that drift with the currents (Falkowski & Raven 1997). Fewer than 25,000 morphologically defined forms are distributed

among at least eight major divisions or phyla. In contrast, nearly all photosynthetic organisms on land belong to a single clade (Embryophyta) that contains approximately 275,000 species (Table 1). Marine phytoplankton constitute less than 1% of Earth's photosynthetic biomass, yet they are responsible for more than 45% of our planet's annual net primary production (Field et al. 1998). Their evolutionary trajectories have shaped trophic dynamics and strongly influenced global biogeochemical cycles. In this paper, we examine the macroevolutionary histories of the major eukaryotic phytoplankton taxa that dominate the contemporary oceans, and consider their relationships to biogeochemical cycles.

ORIGINS OF PHOTOSYNTHESIS AND EUKARYOTIC PHYTOPLANKTON: MOLECULAR EVIDENCE

The origins of photoautotrophy are uncertain. Sedimentary microstructures as old as 3,500 Mega-annum (Ma) have been interpreted as cyanobacteria (Schopf 1993, Schopf 2002), but these reports have been questioned (Brasier et al. 2002). Carbon isotope measurements of reduced carbon in successions as old as 3,800 Ma seem to indicate widespread autotrophy in the oceans (Rosing 1999); however, the processes that led to the isotopic fractionation are not well understood. Perhaps more convincingly, fossil lipid biomarkers indicate that oxygenic photoautotrophs were present in the oceans by ca. 2,800 Ma (Brocks et al. 2003) and by ca. 2,300 Ma they had oxidized Earth's atmosphere (Bekker et al. 2004). Oxygenic photosynthesis subsequently spread to eukaryotes via cyanobacterial endosymbiotic associations that evolved to keep the process localized in membrane-bound organelles called plastids (Yoon et al. 2004). A series of primary, secondary, and possibly even tertiary endosymbiotic associations spread photoautotrophy to five of the eight major extant eukaryotic clades, giving rise to multiple new eukaryotic phyla (Figure 1, see color insert) (Baldauf 2003, Delwiche 1999, Palmer 2003, Yoon et al. 2004).

The earliest photosynthetic eukaryotes arose from one and possibly two successive endosymbiotic events in which the derived organelles were originally photosynthetic bacteria. One clade of early eukaryotes engulfed an ancestral cyanobacterium that was transformed into a plastid. More controversial is the proposal that an earlier, ancestral eukaryote incorporated the antecedent of an extant purple nonsulfur bacterium, which conferred an anoxygenic photosynthetic pathway on the host cell (Taylor 1987). The engulfed bacterium ultimately became the mitochondrion and lost its ability to photosynthesize, perhaps because of environmental oxidation. To accommodate the production of molecular oxygen within this new host-cell complex, the nascent mitochondrion would have operated its electron transport pathway in reverse (Osyczka et al. 2004), thereby giving rise to an oxygen-dependent respiratory electron transport chain with extremely high-energy conversion efficiencies. In this view, the evolution of the only two organelles that originated via endosymbiotic events were "motivated" by photosynthetic carbon acquisition pathways.

This original symbiotic engulfment of a cyanobacterium into a host cell was a “primary” endosymbiotic process. The engulfed cyanobacterium contained a full complement of genes that allowed the organism to replicate itself. The symbiotic association was accompanied by the transfer of coding genes from the cyanobacterial genome into the eukaryotic nucleus. Assuming the genomic composition of extant cyanobacteria is representative of the ancestral symbiont genome, then 90% to 99% of the genes in the nascent plastid were subsequently lost or transferred to the host cell nucleus (Grzebyk et al. 2003, McFadden 1999, Palmer 2003). As a result, although they retain a core set of genes and limited autonomous capabilities for some housekeeping molecular processes, plastids cannot live longer than hours and cannot replicate outside of the host cell.

Three extant phytoplankton phyla (Chlorophyta, Rhodophyta, and Glaucophyta) result from primary endosymbiosis. Various datasets of the eukaryotic host cell (18S ribosomal RNA gene (Figure 1), protein genes (Baldauf et al. 2000), or mitochondria (Gray et al. 1998) indicate that these clades were derived from a common heterotrophic ancestor. Plastid gene phylogenies, such as those inferred from 16S ribosomal genes (Figure 2, see color insert), also show the initial division of the plastid cluster according to the three types of primary plastids, typically surrounded by two membranes: cyanelles, green plastids (chloroplasts), and red plastids (rhodoplasts). Thus, despite their physiological differences, the three phyla may have originated from a single endosymbiotic event. Primary green plastids appear to have differentiated from the other two early in their evolutionary history. The accessory pigment, chlorophyll *b* (*chl b*), is the hallmark of the “green” plastid lineage, which became the forerunner of all chlorophyte algae and (subsequently) all higher plants that colonized terrestrial ecosystems in the Paleozoic. Cyanelles and rhodoplasts have many structural, biochemical, and genetic features in common; they contain chlorophyll *a* (*chl a*) only and have phycobilin pigments located in phycobilisomes, a simple carotenoid composition with zeaxanthin and α -carotene or β -carotene similar to cyanobacteria, and plastid genomes that retain numerous genes lost in chloroplasts.

Secondary endosymbiosis is a process that involves two eukaryotic cells and appears to be unique to plastid evolution. A heterotrophic cell first engulfed an alga with primary plastids. This complex mix of organelles was subsequently “enslaved,” and the core photosynthetic machinery was salvaged and reduced to a new plastid. Secondary endosymbiotic plastids are present in a number of algal phyla. Two of them are characterized by secondary green plastids (Euglenophyta and Chlorarachniophyta, Figure 1). Plastids in four other algal lineages—cryptophytes, haptophytes (including coccolithophores), dinoflagellates (division Dinophyta), and heterokonts (Figures 1 and 2)—originated from a symbiotic association that appears to have differentiated from rhodophytes. Heterokonts include multiple algal classes, such as diatoms (Bacillariophyceae), brown algae (Phaeophyceae), and classes with species that form harmful algal blooms (Raphidophyceae and Pelagophyceae).

TABLE 1 The higher systematic groups of oxygenic photoautotrophs, with estimates of the approximate number of total known species, their distributions between marine and freshwater habitats^a, and the type of plastid and major accessory pigments they contain

Category	Taxonomic group		Known species			Plastids		
	Name		Total	Marine	Freshwater	Type	Accessory pigments ^b	
Empire	Bacteria (= Prokaryota)							
Kingdom	Eubacteria		1,500	150	1,350	N/A	B, Z, β, A	
Subdivision	Cyanobacteria (stricto sensu)							
	(= Cyanophytes, blue-green algae)							
Subdivision	Chloroxybacteria (= Prochlorophyta)		3	2	1	N/A	<i>dvb</i> , Z, α, β	
Empire	Eukaryota							
Kingdom	Protozoa							
Division	Euglenophyta		1,050	30	1,020			
Class	Euglenophyceae					S (green)	<i>b</i> , Dd, Dt, β, N, A	
Division	Dinophyta (Dinoflagellates)							
Class	Dinophyceae		2,000	1,800	200	S (red)	<i>c</i> ₂ , Pe, Dd, Di, Dt, β	
Kingdom	Plantae							
Subkingdom	Biliphyta							
Division	Glaucocestophyta							
Class	Glaucocestophyceae		13	—	13	P (cyan.)	B, Z, α, β	
Division	Rhodophyta		6,000	5,880	120	P (red)	B, Z, β, α	
Class	Bangiophyceae							
Class	Florideophyceae							
Subkingdom	Viridiplantae							
Division	Chlorophyta					P (green)	<i>b</i> , L, N, V, Z, β, α, A	
Class	Chlorophyceae		2,500	100	2,400			
	Prasinophyceae		120	100	20		P (Z missing)	
	Ulvophyceae		1,100	1,000	100			
	Charophyceae		12,500	100	12,400			

EVOLUTION OF EUKARYOTIC PHYTOPLANKTON 527

Division	Bryophyta (mosses, liverworts)	22,000	—	1,000	
Division	Lycopsidea	1,228	—	70	
Division	Filicopsida (ferns)	8,400	—	94	
Division	Magnoliophyta (flowering plants)	240,000	—	—	
Subdivision	Monocotyledoneae	52,000	55	455	
Subdivision	Dicotyledoneae	188,000	—	391	
Kingdom	Chromista				
Subkingdom	Chlorenchia				
Division	Chlorarachniophyta				S (green)
Class	Chlorarachniophyceae	3–4	3–4	—	<i>b</i> , <i>L</i> , <i>N</i> , <i>V</i> , β
Subkingdom	Euchromista				
Division	Cryptophyta				
Class	Cryptophyceae	200	100	100	c_2 , B , A , α
Division	Haptophyta				
Class	Prymnesiophyceae	500	100	400	$c_1/c_2/c_3$, Fu/BF/HF, Dd, Dt, β
Division	Heterokontophyta				
Class	Bacillariophyceae (diatoms)	10,000	5,000	5,000	c_1/c_2 , Fu, Dd, Dt, β
	Chrysophyceae	1,250	800	450	c_1/c_2 , Fu/BF, Dd, Dt, β
	Eustigmatophyceae	12	6	6	Va, V, β
	Phaeophyceae (brown algae)	1,500	1,497	3	$c_1/c_2/c_3$, Fu, Dd, Dt, V, β
	Raphidophyceae	27	10	17	c_1/c_2 , Fu, Dd, Dt, β
	Tribophyceae (Xanthophyceae)	600	50	500	Va, Dd, Dt, β , c_1/c_2
Kingdom	Fungi				
Division	Ascomycotina (lichens)	13,000	15	20	

^aThe difference between the number of marine and freshwater species, and that of known species, is accounted for by terrestrial organisms. Dashes indicate that no species are known (by us) for their particular group in this environment. Abbreviations are as follows. Plastid type: P = primary plastid (cyanelle, red, or green); S = secondary plastid (from the green or red plastid lineage). Accessory pigments: B = bilipigments; *b* = chlorophyll *b*; $c_1/c_2/c_3$ = chlorophyll *c* type 1, 2 or 3; *dhb* = divinyl chlorophyll *b*. Carotenoids: α = α -carotene; β = β -carotene; A = antheraxanthin; Aljalloxanthin; BF = 19'-butanoyloxyfucoxanthin; Dd = diadinoxanthin; Di = diatoxanthin; Dt = diatoxanthin; Fu = fucoxanthin; HF = 19'-hexanoyloxyfucoxanthin; L = lutein; N = neoxanthin; P = prasinoxanthin; Pe = peridinin; V = violaxanthin; Va = vaucheriaxanthin; Z = zeaxanthin. One-digit abbreviations indicate pigments already present in cyanobacteria or primary plastids; two-digit abbreviations indicate pigments appearing in secondary plastids.

^bSources: Van den Hoek et al. (1995), Jeffrey et al. (1997), Paerl et al. (2003).

There is ongoing debate over the number of endosymbiotic events in the evolutionary history of eukaryotic phytoplankton. Early molecular phylogenetic analyses suggested that the two secondary green plastid clades and four secondary red phyla were derived from independent endosymbiosis events. The nuclear and mitochondrial genomes of these two secondary green phyla are not closely related (Figure 1) (Baldauf 2003, Gray et al. 1998). Similarly, nuclear and plastid gene phylogenetic analyses indicate that the cryptophytes, haptophytes, dinoflagellates, and heterokonts arose from independent host cells. Plastid gene phylogenies indicate multiple origins of secondary plastids within rhodophytes (see Figure 2) (Bhattacharya & Medlin 1998, Müller et al. 2001, Oliveira & Bhattacharya 2000, Yoon et al. 2002a), and eukaryotic gene sequence analysis indicates that secondary host cells were unrelated or, at best, that heterokonts and alveolates share an ancient common ancestor (Figure 1) (Baldauf 2003, Baldauf et al. 2000, Bhattacharya & Medlin 1998). However, it has been proposed that secondary endosymbiosis occurred only twice: once in the green algal lineage and once in the red algal lineage (Cavalier-Smith 2003). A single endosymbiotic origin of plastids in the “green” euglenids and chlorarachniophytes seems unlikely, but some phylogenetic studies support the single-event hypothesis for phyla that contain secondary red plastids (Fast et al. 2001, Harper & Keeling 2003, Yoon et al. 2002b). This indicates that all extant basal heterokonts and alveolates must have then lost their plastids to return to the heterotrophic nutritional mode.

Endosymbiotic events transformed both the eukaryotic host and symbiotic cells. The most noticeable impact concerned the composition of accessory photosynthetic pigments (Table 1). Most extant marine cyanobacteria contain only chl *a*, open-chain tetrapyrroles (phycobilins), and two carotenoids (zeaxanthin and β -carotene). However, the cyanobacterial division of Prochlorophyta also contains chl *b* or a divinyl derivative as a major accessory pigment. Within the Eucarya, chl *b* is present only in green plastids (hereafter, the “green” line), whereas phycobilins are present only in red plastids. For that reason, the ancestor of plastids was suggested to have been a cyanobacterium that contained both chl *b* and phycobilins (Tomitani et al. 1999). However, that hypothesis appears to be unlikely because extant prochlorophytes are genetically very distant from plastids (Hess et al. 2001). After primary endosymbiosis, rhodophytes retained the cyanobacterial pigments (but with α -carotene instead of β -carotene), and glaucophytes acquired an additional minor carotenoid. In contrast, primary green plastids greatly diversified in carotenoid pigments; they added four major pigments that absorb light in the wavelength range 400 to 520 nm (versus the less energetic wavelength range of 480 to 580 nm absorbed by rhodophytes). Whereas one may ask if the “primitive” pigment composition of rhodophytes limited the evolution of this phylum, interestingly, accessory pigments diversified in the red plastid lineage after secondary endosymbiosis. The new set of pigments, although specific to secondary red plastids, conferred similar properties to new plastids that mimic those provided by accessory pigments of primary green plastids. Chlorophyllide *c* and its derivatives, which are not present in any extant photosynthetic prokaryotes or in rhodophytes,

absorb light in the 450 to 480 nm range, which nearly overlaps the absorption range by chl *b*. Secondary red plastid carotenoids, some of which are unique to a phytoplankton phylum, absorb light from 400 nm up to 580 nm. We refer to the secondary red plastid phyla that contain chl *c* as the “red plastid lineage.”

EARLY PHYTOPLANKTON EVOLUTION: FOSSIL EVIDENCE

Fossils of probable eukaryotic origin first appear in abundance in rocks dated as approximately 1,700 to 1,900 Ma (Han & Runnegar 1992, Javaux et al. 2001, Knoll 1994). This age should be regarded as a minimum date for eukaryotic diversification because the paleontological record of older strata is sparse; molecular biomarkers suggest that both cyanobacteria and at least stem group eukaryotes existed by 2,700 Ma (Brocks et al. 1999, Summons et al. 1999), and the former, at least, may have evolved earlier (Knoll 2003). The systematic affinities of the earliest eukaryotic fossils are poorly constrained, but by 1,200 Ma, multicellular red algae lived along tidal flats, attached to hardgrounds (Butterfield 2002).

The presence of rhodophytes in mid-Proterozoic rocks places a minimum constraint on the timing of the red-green plastid schism. Reds radiated early as multicellular, benthic constituents of nearshore communities (Xiao et al. 2004). In contrast, early branching greens are planktonic, the paraphyletic “prasinophytes” that still contribute to photosynthesis in open ocean environments (Melkonian & Surek 1995). Xanthophyte fossils in uppermost Mesoproterozoic and Neoproterozoic rocks (Butterfield 2000, German 1990) indicate that secondary endosymbiosis followed relatively closely on the heels of primary events.

The functional as well as phylogenetic schism of reds and greens suggests that early members of the two lineages became adapted for different environmental regimes; the greens proliferated in oligotrophic open oceans underlain by anoxic waters, whereas the reds differentiated in coastal waters where both nutrients and fully oxygenated waters were more abundant (Anbar & Knoll 2002). Cyanobacteria appear to have dominated primary production in early to middle Proterozoic oceans, but by the end of the era (543 Ma), eukaryotic algae had become important constituents of marine ecosystems (Knoll 1989, Knoll 1992, Lipps 1993, Tappan 1980).

Many fossils of Proterozoic (and younger) protists cannot be assigned to extant taxa with any degree of certainty. Closed, organic-walled structures that resemble (at least broadly) dinocysts or prasinophyte phycomata are called “acritarchs,” a grouping that makes them easier to deal with, but not to understand. Acritarchs first appeared as a minor component of the fossil record approximately 1700 to 1900 Ma (Summons et al. 1992, Zhang 1986); a moderate increase in diversity occurred approximately 800 to 900 Ma (Knoll 1994). This diversification coincides with the early stages of Rodinia rifting; however, no firm causal link has been established between the two events (Figure 3, see color insert).

In the Cambrian and Ordovician, eukaryotic phytoplankton underwent a second diversification in concert with the early Paleozoic radiations of marine invertebrates. The affinities of Early Paleozoic phytoplankton remain a subject for debate (Molyneux et al. 1996). Molecular biomarkers indicative of dinoflagellates occur in association with some Cambrian microfossils (Moldowan & Talyzina 1998), but morphological and ultrastructural analyses also show that prasinophyte green algae played a larger role in the continental shelf phytoplankton than they have in more recent times (Colbath & Grenfell 1995, Talyzina & Moczydlowska 2000). Preserved phytoplankton diversity peaked in the mid-Paleozoic and declined rapidly in the Late Devonian to Early Mississippian.

THE RISE OF THE RED LINEAGE

Mesozoic Expansion of the Red Lineage

In the early Mesozoic, the red eukaryotic phytoplankton began to assume a new ecological importance in the marine realm (e.g., Falkowski et al. 2004a,b). Marine prasinophytes declined during the Jurassic and Cretaceous, although this group of green algae is still represented in the oceans today (albeit as a minor constituent of open-ocean communities). A period of transition to red-line dominated primary production occurred in the Triassic to Early Jurassic, ultimately resulting in the ecological dominance of coccolithophores, dinoflagellates, and diatoms in the contemporary ocean.

The first unequivocal dinoflagellates appeared in the fossil record as organic-walled cysts preserved in Middle Triassic continental margin sediments (Stover et al. 1996). Studies of molecular biomarkers indicate that dinoflagellates may have existed as far back as the Neoproterozoic (Moldowan & Talyzina 1998, Summons & Walter 1990); however, these biomarkers did not become prominent constituents of marine bitumens until the Triassic (Moldowan et al. 1996, Moldowan & Jacobson 2000), when microfossils more clearly document their expansion and radiation (Fensome et al. 1996, Stover et al. 1996) (Figure 3).

The calcareous nannoplankton (dominated by coccolithophorids) were the second group in the red lineage to radiate in the fossil record. They originated in the Late Triassic (Bown et al. 2004) (Figure 3) at about the same time that molecular biomarkers of coccolithophorids became common (Moldowan & Jacobson 2000). The earliest nannoplankton have been identified in Carnian sediments from the southern Alps (Bown 1998, Janofske 1992) and Nevada (F. Tremolada, personal communication).

The silica-encased diatoms were the last of the three major groups to emerge in the Mesozoic. The siliceous diatom frustules are highly soluble compared with other siliceous fossils (e.g., radiolaria and sponge spicules), which possibly imparts a preservational bias to the fossil record of diatom origin. Reports of diatom frustules in Jurassic sediments (Rothpletz 1896) have proved difficult to replicate by later workers, although molecular biological clock estimates (Medlin et al. 2000)

and molecular biomarkers (Moldowan & Jacobson 2000) indicate that diatoms may have evolved earlier, but remained minor components in the marine realm until the Cretaceous. The first unequivocal fossil records of diatoms document radiations in the Early Cretaceous oceans (Harwood & Nikolaev 1995). Diatom morphologies in the Early Cretaceous were dominated by cylindrical and long-cylindrical forms that show very little variation (Gersonde & Harwood 1990, Harwood & Gersonde 1990); the similarity among these early diatom morphologies argue against a pre-Mesozoic origin (Harwood & Nikolaev 1995). Late Cretaceous diatoms were dominated by discoidal and biddulphioid frustule morphologies (Harwood & Nikolaev 1995). Diatoms were present in nonmarine environments by 70 million years ago (mya) (Chacon-Baca et al. 2002).

Regardless of the exact timing of the evolutionary origins of coccolithophores, dinoflagellates, and diatoms, fossil and biomarker data document the major expansion of all three groups in the Mesozoic (Bown et al. 2004, Grantham & Wakefield 1988, Harwood & Nikolaev 1995, Moldowan & Jacobson 2000, Stover et al. 1996) (Figure 3). They began their evolutionary trajectories to ecological prominence as the supercontinent Pangea began to break apart in the Late Triassic to Early Jurassic (~200 Ma), which marked the opening phase of the current Wilson cycle of continental breakup, dispersal, and reassembly (see, The Role of the Wilson Cycle below). Sea level rose as Pangea fragmented and the Atlantic Ocean basin widened, flooding continental shelves and low-lying inland areas (Figure 3). In addition, the fragmentation of the continents and creation of a new ocean basin produced an increase in the total length of coastline where many plankton lived. Nutrients (such as phosphate) that were previously locked up in the large continental interior of Pangea were transported to newly formed shallow seas. At the same time, diversities increased in the three groups of eukaryotic phytoplankton, and in marine invertebrates, paralleling a long-term increase in sea level that began in the Early Jurassic (Haq et al. 1987, Vail et al. 1977) (Figure 3). Greater nutrient availability coupled with expanded habitat area may well have contributed to the radiation of phytoplankton that lived along continental margins. Accordingly, the diversities of eukaryotic phytoplankton of the red lineage parallel sea-level rise through the Mesozoic (Figure 3). In contrast, short-term (1-Myr scale) sea-level changes may have resulted in species turnover events, but had very limited impact on the large-scale evolutionary history of phytoplankton clades.

Life-cycle strategies may also have been an important component that favored the radiation of the red lineage as continental shelves flooded and epicontinental seas became widespread in the Jurassic. Dinoflagellates, coccolithophorids, and diatoms produce resting stages. After a bloom, a small fraction of the phytoplankton population becomes arrested in a specific stage of the cell's life cycle in which the production of cell armor increases, and the cell sinks to the seafloor until conditions become favorable to bloom (usually the following year). The timing of the bloom depends on environmental conditions such as ocean stratification and day length. The resting stage is associated with gamete formation and gene exchange in the planktonic portion of the life cycle. This life-cycle strategy requires shallow

marine areas and also promotes genetic isolation by reducing the gene flow. Gene transfer, which can occur through sexual recombination, lateral vectors (such as viral infection), or both, is highly attenuated in benthic stages. Over relatively short periods of time, genetic isolation may have increased the tempo of evolution and phenotypic selection, processes that have been observed in contemporary phytoplankton assemblages (Medlin et al. 1997).

Cenozoic Expansion of Diatoms

Bolide impact at the Cretaceous/Tertiary boundary (65 Ma) caused major extinctions (Alvarez et al. 1980) that are recorded in the fossil records of the coccolithophores and, to a lesser extent, the diatoms and dinoflagellates (Figure 3). The environmental factors that favored the expansion of the red lineage through the Mesozoic allowed these phytoplankton to repopulate the marine realm after the Cretaceous/Tertiary boundary (K/T) mass extinction event. Dinoflagellates and calcareous nannoplankton recovered to preextinction diversity levels by the earliest Eocene (~55 mya), only to decline through the rest of the Cenozoic as long-term sea level began to fall in the mid-Paleogene and the extent of flooded continental areas decreased. Among fossilizable taxa, modern dinoflagellate species diversity has declined to levels comparable to the earliest Middle Jurassic, whereas modern coccolithophorid species diversity has declined to Late Jurassic levels.

In contrast to the other phytoplankton, diatom diversity has increased through the Cenozoic, despite falling sea level. Two pulses of diversification occurred in diatoms: the Eocene/Oligocene boundary interval and the middle to late Miocene. The latter was accompanied by a substantial radiation among pennate species (Strelnikova 1991). Conditions that may have favored the expansion of diatoms in the Cenozoic are discussed in the following section.

SELECTION PRESSURES AND ADAPTATIONS

Resource Acquisition

In contrast to most species of dinoflagellates and coccolithophores, diatoms frequently form extensive blooms along continental margins and in upwelling regions of the contemporary ocean. These organisms are responsible for approximately 40% of the net primary production and more than 50% of the organic carbon that is exported to the ocean interior (Falkowski et al. 2003b). Planktonic diatoms have evolved a nutrient storage vacuole that retains high concentrations of nitrate and phosphate (Raven 1997). The storage vacuole allows diatoms to acquire pulses of inorganic nutrients, which can deprive competing taxa of these essential resources, overcome light-dependent nutrient uptake in mixing systems, or both. The storage capacity of the vacuole is sufficient to allow two to three cell divisions without the need for external nutrient resources. Consequently, diatoms thrive best in regions where nutrients are supplied with high pulse frequencies.

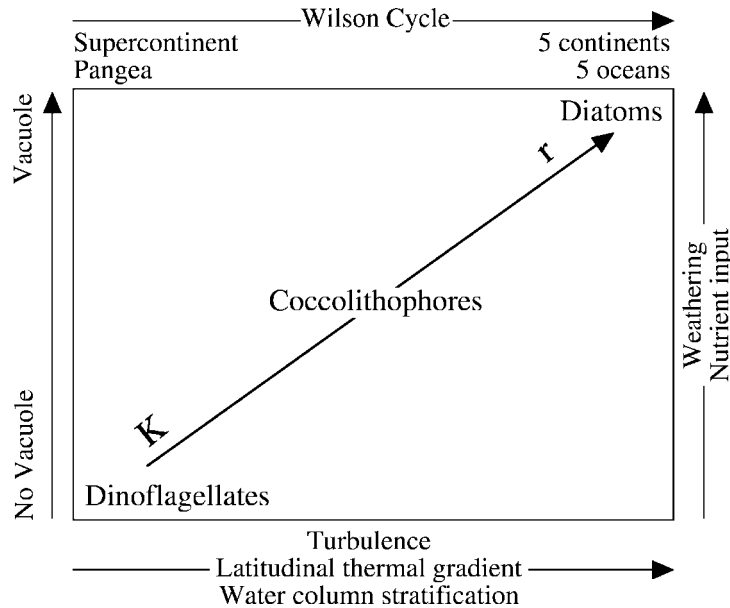


Figure 4 Models based on resource acquisition strategies (e.g., Grover 1988, Litchman E, Klausmeier CA, Miller JR, Schofield OM, Falkowski PG in review, Tilman 1977, Tozzi et al. 2004) suggest that diatoms dominate when brief periods of water-column stability are punctuated by high turbulence, whereas coccolithophores and dinoflagellates dominate when the water column is more stably stratified. After Tozzi and others (Tozzi et al. 2004).

Competition among diatoms, coccolithophores, and dinoflagellates has been modeled by application of resource acquisition strategies (e.g., Grover 1991; Litchman E, Klausmeier CA, Miller JR, Schofield OM, Falkowski PG in review; Tilman 1977; Tozzi et al. 2004). The results of these models suggest that diatoms dominate when brief periods of water-column stability are punctuated by high turbulence, such as storm events (Figure 4). In contrast, coccolithophores and dinoflagellates dominate when the water column is more stably stratified. In theory, competitive exclusion could occur if equilibrium conditions were reached. In reality, the coexistence of two or more taxa competing for a single resource is a consequence of the dynamically unstable nature of aquatic ecosystems (Li 2002, Siegel 1998). Margalef (1994) recognized these fundamental differences in physiology and proposed that competition among the three major red lineage taxa could be related to upper-ocean turbulence and the supply of nutrients. The so-called Margalef mandala can be extended over geological time (Prauss 2000) to infer selection processes that led to the early rise of dinoflagellates and coccolithophorids in the relatively stable conditions of the Mesozoic, followed by the rise of diatoms in the Cenozoic.

Increasing latitudinal thermal gradients and decreasing deep-ocean temperatures have contributed to greater vertical thermal stratification through the latter half of the Cenozoic, which increased the importance of wind-driven upwelling and mesoscale eddy turbulence in providing nutrients to the upper ocean. The ecological dominance of diatoms under certain sporadic mixing conditions suggests that their long-term success in the Cenozoic probably can be attributed in part to an increase in event-scale turbulent energy dissipation in the upper ocean (Falkowski et al. 2004a). Sporadic nutrient influx to the euphotic zone may favor diatoms over coccolithophores and dinoflagellates, and a change in concentration and pulsing may favor small diatoms over large diatoms. As a result, a significant decrease in the average size of diatoms occurred in the Cenozoic. Periods of change were concentrated in the middle to late Eocene and early to middle Miocene (Finkel, Katz, Wright, Schofield, & Falkowski submitted).

Silica Bioavailability

Diatoms precipitate orthosilicic acid in a protein matrix to form extremely strong, structurally intricate biogenic opal shells called frustules. The modern oceans are undersaturated with respect to silica, which is largely the result of the evolution and ecological success of diatoms in removing this element from the dissolved phase, especially in the latter half of the Cenozoic (Conley 2002). Eighty percent of the silica in the oceans is derived from chemical and biological weathering of continental rocks (De La Rocha et al. 2000); the annual net riverine flux is 5.0 Tmol of silica per year (Tréguer et al. 1995). Sustaining the silica flux on geological timescales requires that fresh rock surfaces continuously become exposed to the soil interface, a process that is perpetuated by erosion. The rate of nutrient flux to the oceans on multimillion-year timescales is determined in part by continental elevation. Both orogeny and regression have characterized nearly all of the continents during the Cenozoic, which has increased nutrient fluxes (including silicic acid) (Maldonado et al. 1999) and facilitated diatom expansion (Falkowski et al. 2004a,b). An additional loop in the silica cycle that developed in the Cenozoic also may have accelerated the success of diatoms. The loop involves the coevolution of mammals, grasses, and diatoms. Grasses extract silicic acid from groundwater in soils and store it in opal phytoliths (Conley 2002). Silica can constitute as much as 15% of the dry weight of grasses (Alexandre et al. 1997, Bartoli 1983, Rapp & Mulholland 1992), and phytolith dissolution can release soluble silica two times more efficiently than silicate weathering (Alexandre et al. 1997).

Grasses originated in the Cretaceous, but remained sparse until the Eocene/Oligocene boundary (33.7 Ma) (Kellogg 2000, Retallack 2001), when global climates became more arid as a result of major glaciation in the Antarctic. As grasslands expanded, grazing ungulates evolved and displaced browsers (Janis & Damuth 2000). Hypsodont (high-crown) dentition in ungulates was selected over the brachydont (leaf-eating) dentition in browsing mammals, which coincided with the widespread distribution of silica-rich phytoliths and grit in grassland

forage (Retallack 2001). The rise of grazing ungulates and the radiation of grasses may have acted as a biologically catalyzed silicate weathering process (Falkowski et al. 2004a,b). Phytolith diversity and abundance has increased since the late Eocene (Jacobs et al. 1999, Retallack 2001); almost certainly grass-mediated silica mobilization from soils increased as the grasses radiated. The subsequent transfer of silica to the oceans (primarily via riverine transport) increased the bioavailability of silica for diatom growth (Falkowski et al. 2004a,b). Accordingly, diatom species diversity, and presumably abundance, increased dramatically at the Eocene/Oligocene boundary (Figure 3). A major expansion of grasslands in the Neogene (Retallack 1997, Retallack 2001) was accompanied by a second pulse of diatom diversification at the species level (Falkowski et al. 2004a,b).

Armor

We can infer the evolutionary trajectories of all three major red lineage clades that appear to have dominated the eukaryotic phytoplankton community since the Mesozoic because they have fossilizable cell walls that also provide armor. This armor likely protected the phytoplankton from grazers long enough to for the phytoplankton to form blooms (Banse 1992). Although the composition of the cell walls differs markedly among dinoflagellates, coccolithophorids, and diatoms, grazing by zooplankton may have provided a common evolutionary selection pressure. Unfortunately, virtually no fossil record exists for major modern pelagic zooplankton groups; chitinous crustaceans (e.g., copepods and euphausiids) decompose rapidly in the sediments, and virtually all soft-bodied organisms such as salps decompose in the water column before they reach the sediments. The potential role of cell walls as armor against grazing has long been debated (Smetacek 1999, 2001). The strength and flexibility of diatom frustules makes fracturing them a challenge for invertebrates; in fact, diatoms can pass through a copepod gut intact (Hamm et al. 2003). The chitinous teeth of copepods have a siliceous coating that provides significant compressive strength, and mandible muscles in these crustaceans are highly developed. This feature is a clear example of adaptive evolution between predator and prey in pelagic ecosystems (Adams 2001). However, if diatoms are consumed, zooplankton greatly facilitate the dissolution of the frustule (Bidle & Azam 1999).

Coccolithophores are grazed, but the nutritional benefit derived from ingesting a cell consisting of 30% calcium carbonate is lower than that derived from ingesting a naked cell of the same size. Indeed, zooplankton avoid coccolithophorids if presented with optional, unarmored food sources (Falkowski and Wyman, unpublished data). In addition to armor, thecate dinoflagellates (and some diatoms) have evolved a strategy of vertical migration; they obtain nutrients below the pycnocline at night and rise to the upper portion of the euphotic zone during the day to optimize photosynthesis (Kamykowski 1981, Villareal et al. 1993). This migration strategy is out of phase with that of many zooplankton grazers (Banse 1964).

Ocean Chemistry

Secular changes in seawater chemistry also appear to have influenced phytoplankton evolutionary trajectories. For example, trace elements (including iron, copper, zinc, and manganese) play essential roles in mediating critical biochemical reactions in all phytoplankton. The bioavailability of these elements in seawater is strongly dependent on redox state (Whitfield 2001). Algae with green plastids have substantially higher quotas for iron, zinc, and copper (i.e., Fe:P, Zn:P, and Cu:P ratios) than do red eukaryotes, whereas the latter have higher quotas for cadmium, cobalt, and manganese (Quigg et al. 2003). Furthermore, the redox state of the oceans may discriminate between red and green plastid lineages with respect to fixed nitrogen preferences (Anbar & Knoll 2002, Falkowski & Raven 1997, Litchman E, Klausmeier CA, Miller JR, Schofield OM, Falkowski PG in review), as well as the availability of phosphate. Members of the green plastid lineage tend to have higher N/P ratios than members of the red plastid lineage (Falkowski et al. 2004b). Hence, the form and availability of macronutrients and trace metals have the potential to be strong selective agents that favor red or green plastid containing taxa.

The Archean biosphere was anoxic, and its initial oxidation in the Paleoproterozoic Era introduced oxygen primarily into the surface mixed layer of the oceans. Complete oxygen depletion appears to have remained common beneath the pycnocline, and sulfidic deep waters were widespread (Canfield) (Figure 3). Under these conditions, early algae likely competed best in the better-oxygenated coastal regions, where rivers delivered essential metals (Anbar & Knoll 2002). As noted above, the evolutionary divergence of red and green plastids took place in the context of this redox heterogeneity and may have contributed to the different evolutionary trajectories of rhodophytes and early chlorophytes. Increasing oxidation of ocean waters may have facilitated the expansion of algae across shelves in latest Neoproterozoic times; undoubtedly interactions with evolving animals also contributed to Cambrian and Ordovician phytoplankton diversification (Butterfield 1997).

Black shales are common in Proterozoic marine successions, which indicates oxygen depletion beneath surface water masses in the oxygen-minimum zone (Shen et al. 2002, Shen et al. 2003); black shales also occur episodically through much of the Paleozoic (Arthur & Sageman 1994). Deep-water anoxia may have been particularly pronounced near the end of the Permian (Isozaki 1997). The expanded oxygen-minimum zone persisted through the Early Triassic (Twitchett 1999, Wignall & Twitchett 2002), and may have altered the distributions of many trace elements within the oceans (Whitfield 2001a). Ocean anoxia increases the availability of Fe, Mn, P, and ammonium and decreases the availability of Cd, Cu, Mo, Zn, and nitrate; hence, the green lineage may have been favored over the red lineage at times when subsurface reducing conditions prevailed.

A secular shift in ocean redox conditions in the early Mesozoic changed trace metal availability in the oceans and exerted a selective pressure that favored the red lineage by better meeting their metal requirements (Falkowski et al. 2004a,b).

The last major occurrence of large concentrations of the green algal prasinophytes was in the Early Jurassic, when black shale deposition and ocean anoxia appears to have been widespread (Falkowski et al. 2004a,b). As deep-ocean oxygenation became increasingly permanent through the Mesozoic, Cd, Cu, Mo, Zn, and nitrate availability increased, which allowed the red lineage to expand (Anbar & Knoll 2002, Falkowski et al. 2004a,b). Temporal changes in the availability of redox-sensitive trace metals are consistent with the biological transition to red-lineage dominance of phytoplankton (Falkowski et al. 2004a,b). Thus, long-term changes in ventilation of the world's oceans ultimately appear to have played a significant role in the rise of the red lineage during the Mesozoic.

The Mesozoic oceans occasionally were punctuated by widespread organic carbon-burial events associated with the short-lived (<1 myr) Oceanic Anoxic Events (OAEs) (e.g., Arthur & Sageman 1994). These events briefly altered ocean redox conditions, but the effects were relatively short-lived. The biological impact of OAEs is debated (e.g., Leckie et al. 2002 versus Bown et al. 2004) despite the substantial effort dedicated to examining the phytoplankton and zooplankton communities across these carbon-burial events (e.g., Erbacher & Thurow 1997, Leckie et al. 2002, Roth 1987). Once the red lineage garnered a more secure ecological advantage in the Late Triassic, the fossil records suggest that the OAEs only had a minor influence on the evolutionary trajectories of eukaryotic phytoplankton (Bown et al. 2004, Falkowski et al. 2004a).

THE ROLE OF THE WILSON CYCLE

The radioactive decay of elements within Earth's core produces heat that dissipates to the planet's surface through convection and conduction. Near the surface, the thin oceanic crust conducts heat about three times more efficiently than the thicker continental crust. The differential dissipation of radiogenic heat between oceanic basalts and continental crust leads to the buildup of thermal energy below a fully assembled supercontinent, which causes the continental crust to thin and eventually to fracture and rift apart. A new ocean-spreading center and ocean basin form between the continental fragments. Heat-driven convection in the mantle below the lithosphere drives the tectonic plates apart with the fragmented continents attached, and new oceanic crust forms at the intervening spreading center. As it ages, the oceanic crust becomes cooler and denser and eventually subsides as it moves away from the spreading center. When this old crust becomes so dense that it subsides below the adjacent, relatively low-density continental crust, a new subduction zone is created and the ocean basin is consumed as the whole process reverses itself and the continents reassemble. Named after its conceptual discoverer, J. Tuzo Wilson (Wilson 1966), this episodic breakup, dispersal, and subsequent reassembly of supercontinents has become known as the Wilson Cycle, and it occurs over approximately 300-Myr to 500-Myr intervals (e.g., Fischer 1984, Rich et al. 1986, Valentine & Moores 1974, Worsley et al. 1986).

The Wilson Cycle and Evolutionary Trajectories

Several studies have drawn attention to the correlation between evolutionary pulses in the marine realm and the Wilson Cycle (e.g., Damsté et al. 2004, Fischer 1984, Rich et al. 1986, Valentine & Moores 1974, Worsley et al. 1986). Myriad studies since these early publications provide the foundation for speculating on causal rather than casual linkages for the phytoplankton response to the Wilson Cycle.

Global species diversity reflects both the packing of taxa within communities and the distribution of suitable habitat area (MacArthur & Wilson 1967, Rosenweig 1995). A geological proxy for the former is provided by estimates of within-assemblage diversity through time (e.g., Bambach 1977), whereas paleobiogeographic analyses gauge the contribution of the latter. Diversity increases correlate with continental rifting during early iterations of the Wilson Cycle. Acritarchs appear to have radiated as Rodinia rifted in the Late Proterozoic, and diversified again in the Early Paleozoic as Pannotia rifted (Figure 3). Thus, continental separation may have played a role, along with the ecological drivers that govern within-assemblage diversity, in promoting Cambro-Ordovician phytoplankton (and marine invertebrate [Sepkowski 1997; Bambach 1999]) expansion.

Sea-level rise and flooded continental area also are highly correlated with increasing diversity of Mesozoic calcareous nannoplankton (e.g., coccolithophorids) and dinoflagellates (Figure 5), as well as with their declining diversities in the Cenozoic oceans. Although flooded continental area is a small percentage of the total oceanic area suitable for phytoplankton, the shallow seas appear to have contributed proportionally more to niche space because of high nutrient input, high rates of primary production, and habitat heterogeneity. Flooded continental area provides variable, high-nutrient habitat by creating additional upwelling zones and increasing turbulence and nutrient suspension from below the thermocline. In addition, terrestrial nutrient input likely increases because nutrients that were previously sequestered in the large supercontinent interior are more readily transported to the newly opened, nearby oceans. We note that flooded continents increase the availability of fossiliferous sediments and have the potential to impart a taphonomic and sampling component to diversity compilations. This bias may be most pronounced in the older record because most pre-Jurassic ocean crust has been destroyed.

A simple equation captures the empirical relationship between long-term sea level change and diversities in calcareous nannoplankton, dinoflagellates, and diatoms (Figure 5); this equation provides correlation coefficients, but is not a predictor of sea level based on phytoplankton diversities. Although accurate reconstruction of diversities is inevitably biased by differential preservation and the problem of defining species based on morphologic characters, our approach provides an estimate of the relationship between phytoplankton richness (R) and sea level (meters) that solves for coefficients that link the diversity of phytoplankton taxa to change in habitat area caused by sea level change. This relationship is defined as:

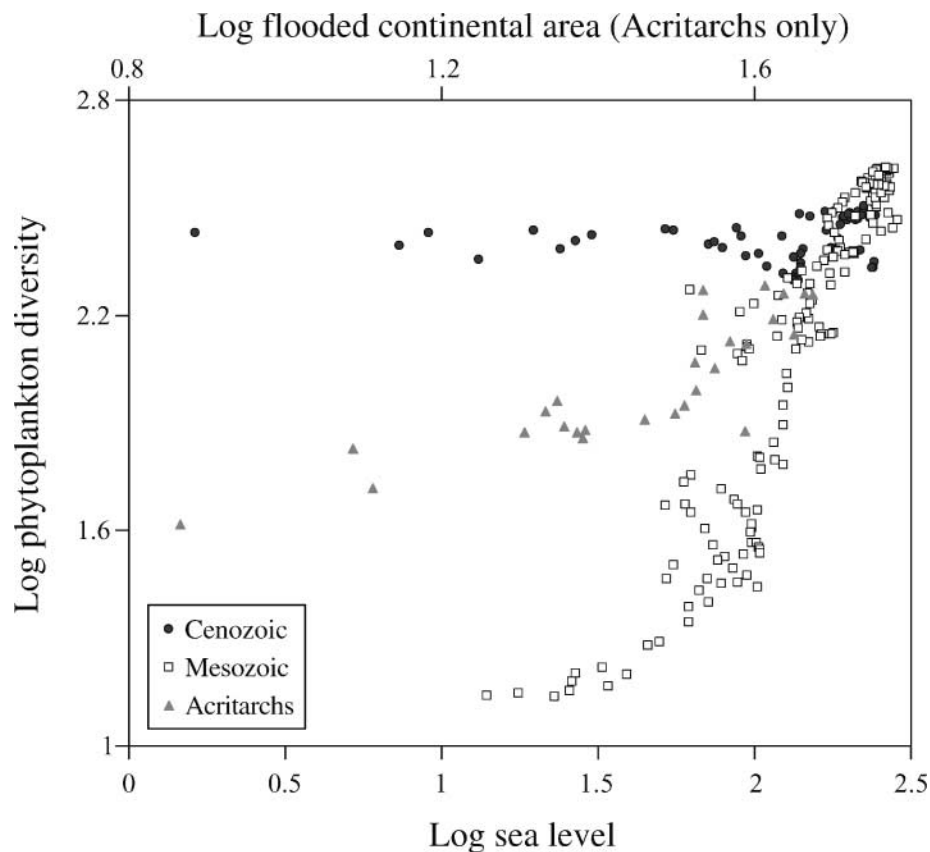


Figure 5 Phytoplankton diversity (sources as in Figure 3) as a function of flooded continental area in the Paleozoic (acritarch genera) and sea level in the Mesozoic (calcareous nannoplankton species + dinoflagellates species). The radiation in diatom species diversity alters the relationship between phytoplankton diversity (calcareous nannoplankton species + dinoflagellate species + diatom species) and sea level change in the Cenozoic. Sea level was translated to obtain positive values. Timescales are as in Figure 3.

$$-0.29 R_{\text{diatoms}} + 0.42 R_{\text{nannos}} + 0.59 R_{\text{dinos}} + 25.4 = \text{sea level} \quad (r^2 = 0.82) \quad (1)$$

Our analysis suggests that whereas calcareous nannoplankton and dinoflagellate diversities are highly correlated to sea level, diatom diversity responds to other environmental factors (see, Selection Pressures and Adaptations above) and has rapidly increased over the past approximately 35 myr.

The tectonic processes that drive the Wilson Cycle not only affect available niche space, but also affect ocean chemistry. As seawater cycles through mid-ocean ridges, magnesium is removed and calcium is added. Total ridge length and

seafloor spreading rates can change Mg/Ca ratios in seawater. As a result, high Mg/Ca ratios tend to occur during times of supercontinent assembly, when ridge length is shortest, characterized by deposition of aragonite and high-Mg calcite (called “aragonite seas”). Low-Mg calcite deposition tends to characterize times of continental breakup (called “calcite seas”) (Hardie 1996, Sandberg 1975). Low-Mg/Ca and high-Ca⁺² concentration in seawater favors calcification in certain groups of marine organisms (including coccolithophores), which results in a correspondence between these organisms and “calcite sea” intervals (Stanley & Hardie 1998). This relationship is illustrated by the expansion of coccolithophores in the Mesozoic calcite seas (Figure 3), along with other low-Mg calcifiers among marine invertebrates. The massive Cretaceous coccolith chalks (e.g., the White Cliffs of Dover) were deposited on continental shelves when margins were flooded, Mg/Ca ratios were low, and dissolved Ca⁺² concentrations in seawater were high. This correlation further links the expansion of coccolithophores to the opening phase of the current Wilson Cycle. Chalk deposition continued in the Paleocene after the K/T extinctions, but as the Mg/Ca ratio increased through the Cenozoic, the degree of calcification in coccoliths declined, and coccolith size decreased (Bukry 1971, Houghton 1991).

Bottom-Up Control of Marine Invertebrate Fauna

In his classic essay “Seafood Through Time,” Bambach (1993) identified a series of changes in late Mesozoic and Cenozoic marine faunas—increases in abundance and mechanical strength of top predators, mean size of marine invertebrates, and mean rates of energy consumption. These changes all require a greater nutritional supply to marine life. Bambach (1993, 1999) suggested that the necessary nutrients were supplied by angiosperm-facilitated increases in erosional runoff from continents, runoff that would have been further augmented by higher erosion rates associated with increasing continental elevations (see above “Silica Bioavailability”). As an additional hypothesis, we propose that the Wilson Cycle and the evolutionary shifts in phytoplankton community composition, in conjunction with increases in primary production and the quantity and quality of export production in the Phanerozoic seas, strongly influenced marine invertebrate faunal evolution.

Marine invertebrate faunal diversity (Bambach 1999) is highly correlated with phytoplankton diversity and community composition (Figure 6), but poorly correlated with flooded continental area ($r^2 = 0.14$) and sea level ($r^2 = 0.05$). An increase in net primary production increases both the availability of organic matter that can be transferred to higher trophic levels in marine invertebrates and the potential to export food to the seafloor (Falkowski et al. 2003a). The fossil record indicates that an evolutionary change in phytoplankton diversity and community composition is a predictor of change in the richness in marine invertebrate genera: (a) diatom genera richness is highly correlated with Cenozoic invertebrate richness ($r^2 = 0.75$); (b) the combined diversity of calcareous nannoplankton and dinoflagellates is highly correlated with Mesozoic invertebrate diversity

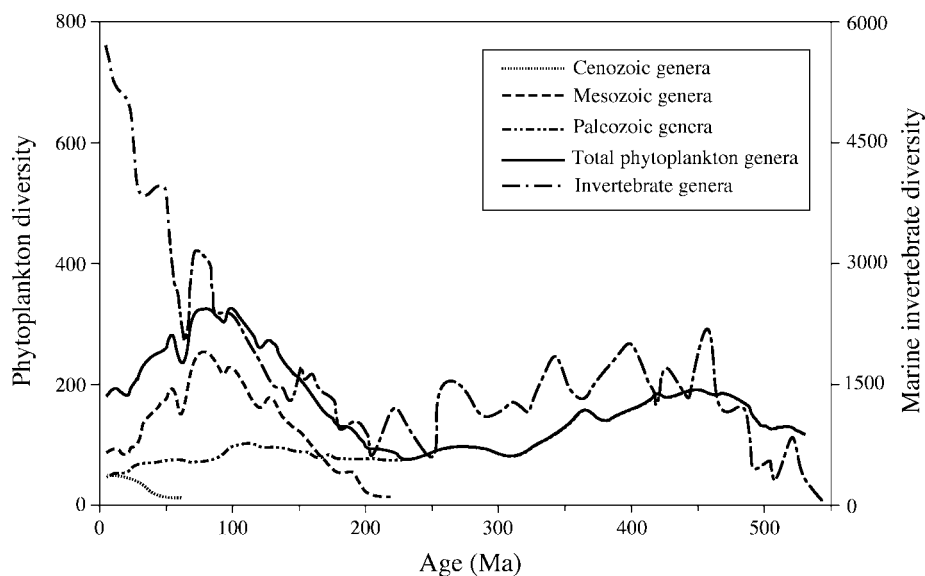


Figure 6 Marine invertebrate diversity (genera; Bambach 1993) and phytoplankton diversity (as in Figure 3) over the Phanerozoic. Timescales are as in Figure 3.

($r^2 = 0.89$); and (c) a weak correlation exists between the diversity of Paleozoic marine invertebrates and the diversity of the acritarchs ($r^2 = 0.12$) (Figure 6).

The radiation of diatoms in the Cenozoic demarcates a large change in food-web structure of the Phanerozoic oceans, which altered the relationship of total phytoplankton diversity to flooded continental area and sea level that had persisted through the Paleozoic and Mesozoic (Figure 5). Total phytoplankton diversity is positively correlated with invertebrate diversity in the Paleozoic and Mesozoic ($r^2 = 0.53$), but becomes inversely related to invertebrate diversity in the Cenozoic ($r^2 = 0.61$). This pattern indicates that the transitions from the prasinophyte/acritarch-dominated Paleozoic ocean to the nannoplankton/dinoflagellate-dominated Mesozoic ocean to the diatom-dominated Cenozoic ocean were likely associated with changes in total primary production, nutritional quality, export production efficiency, and food availability for heterotrophic consumers.

The linear relationship between phytoplankton and invertebrate diversities can be used to infer changes in food-web structure and efficiency of trophic transfer of primary production into invertebrate species over time. This comparison highlights an increase in the number of invertebrate species relative to phytoplankton species through the Phanerozoic (Table 2): (a) each Paleozoic phytoplankton genus is associated with five invertebrate genera; (b) each Mesozoic dinoflagellate genus and nannoplankton species is associated with 7 and 14 invertebrate genera, respectively; and (c) each Cenozoic diatom genus is associated with 59 invertebrate genera. This large change in the richness of invertebrate genera relative to the

TABLE 2 Invertebrate diversity supported per phytoplankton species or genera (the slope) over different time intervals^a

Taxa	Time period	Slope	SE ^b	Intercept	SE ^b	r ²
Diatom genera	Cenozoic	59.0	12.1	2308.0	418.6	0.75
Nannoplankton sp.	Mesozoic	14.5	1.3	707.5	100.4	0.85
Dinoflagellate genera	Mesozoic	6.9	0.6	844.1	85.6	0.86
Nannos + Dinos	Mesozoic	4.9	0.4	766.1	79.9	0.89
Acritarch genera	Paleozoic	5.2	2.3	454.1	322.9	0.12
Sum	Phanerozoic	9.0	1.7	187.4	316.0	0.27

^aInvertebrate diversity (y) is estimated as a linear function of phytoplankton diversity (x) \cdot slope + intercept. Diversity of all groups is represented by number of genera, except calcareous nannoplankton diversity, which is represented by number of species. Data from sources outlined in caption for Figure 3.

^bSE = standard error.

phytoplankton species and genera may represent an increase in the relative biomass of each of the phytoplankton species caused by an increase in primary production, an increase in the amount of primary production that is exported, or both. In part, the increasing ratio of preserved invertebrate to phytoplankton taxa also reflects the increasing richness of specialized predators through time; this relationship is another consequence of increasing primary production in the oceans, or increasing biological availability of primary production to consumers, or both (Bambach et al. 2002). In the contemporary oceans, diatoms are the major phytoplankton taxa contributing to export production (Dugdale et al. 1998). The increased export efficiency associated with the ecological success of marine diatoms most likely contributed to the increase in marine invertebrate diversity, size, and rate of energy consumption.

Evolutionary Tempo of Marine Phytoplankton

We compare evolutionary rates among different taxonomic groups based on background rates of extinction and origination normalized by species richness in the fossil record (Table 3). The results of this analysis show a twofold to fourfold decrease in the average longevity of the calcareous nannoplankton, dinoflagellates, and diatom species from the Mesozoic to the Cenozoic. Using a similar approach, Knoll (1994) described an increase in morphological diversity and a decrease in average species longevity in the acritarchs through the Proterozoic into the early Cambrian, and Barron (2003) documented relatively short longevities (~ 3 myr) in marine diatoms over the past 18 myr from high-resolution records in the Pacific and Southern Oceans. These results highlight the continuing increase in evolutionary tempo of phytoplankton. Extinction rates in dinoflagellates and calcareous nannoplankton have exceeded origination rates through the Cenozoic, which has resulted in declining diversities.

TABLE 3 Estimates of species and genera duration (in Ma \pm 1 SE) for different phytoplankton groups

	Cenozoic	Mesozoic
Diatom species	40 (\pm 6)	
Diatom genera	46 (\pm 1)	100 ^a
Dinoflagellate species	14 (\pm 1)	22 (\pm 3)
Dinoflagellate genera	30 (\pm 4)	73 (\pm 6)
Nannoplankton species	11 (\pm 1)	49 (\pm 6)
	Paleozoic	Proterozoic
Acritarch species cohort ^b	8	102–1960

^aSpecies and genera duration was calculated as $1/(E/R\Delta T)$, where E is the number of species extinctions, R is species richness, and ΔT is the duration of the time period, with 1 standard error (SE) in parentheses. To get an estimate of background duration, the middle 50% of the data was used to calculate the average species duration (and 1 SE) for each time period. Data for diatom species are from Spencer-Cervato (1999), diatom genera are from Harwood & Nikolaev (1995), dinoflagellates are from Bujak & Williams (1979), nannoplankton from Bown et al. (2004). Because of a small sample size, the duration of Mesozoic diatom genera was determined by a sum of all the extinctions over the Mesozoic and the average R for the whole time interval.

^bAcritarch species durations were calculated by cohort analysis by Knoll (1994).

THE ROLE OF PLANKTON IN BIOGEOCHEMICAL CYCLES

Geological and biological processes modify atmospheric and seawater chemistry through time and influence global climates. Submarine and subaerial tectonics in combination with erosional processes are the primary suppliers of the major elements in geochemical cycles; the oxidation and reduction processes that alter mobile elemental reservoirs are biologically mediated. Hence, geological and biological processes together form feedback loops in various biogeochemical cycles.

As we have shown in the preceding sections, changing environmental conditions selected for different plankton groups through Earth's history. In turn, phytoplankton have modified various aspects of the environment through time. Perhaps the most notable example of this relationship is the role that plankton played in the oxygenation of Earth's atmosphere and oceans through the evolution of oxygenic photosynthesis. Increasing oxygen levels led to the oxidation of inorganic substrates, particularly iron and sulfur, which altered seawater chemistry. In turn, primary production became iron limited as the result of iron oxidation in the oceans. In this section, we explore these types of biogeochemical interactions that have left clues preserved in long-term geological records.

Phytoplankton and the Carbon Cycle

The expansion of the red lineage of phytoplankton that began in the Mesozoic had an impact on the long-term carbon cycle, in part by altering the distribution of carbonate and organic carbon buried on the seafloor. Prior to the Mesozoic, most marine calcifying organisms lived in shallow coastal and shelf regions. Carbonate deposition was concentrated in these areas as a result, and deposition of pelagic carbonates was minimal. Two groups of carbonate-secreting plankton successfully competed for limited carbonate resources and expanded in the Mesozoic oceans—coccolithophores, with their calcitic-plated armor, and planktonic foraminifera, with their carbonate tests. As these two groups radiated, the loci of marine carbonate deposition gradually expanded from shallow shelf areas to the deeper ocean (Southam & Hay 1981) (Sibley & Vogel 1976) and the carbonate compensation depth (CCD) deepened (e.g., Wilkinson & Algeo 1989). Pelagic carbonate sedimentation has come to dominate as sea level and shelf area has declined since the Late Cretaceous, and the pelagic carbonate reservoir has increased at the expense of the shallow-water carbonate reservoir since the Mesozoic (Wilkinson & Algeo 1989).

At the same time, the expansion of marine phytoplankton in the Mesozoic resulted in greater export production through time (e.g., Bambach 1993) (see above). The newly-emerged eukaryotic phytoplankton efficiently exported organic matter, and the newly formed Atlantic Ocean margins increased the potential storage area for that organic matter. Substantial amounts of organic carbon were sequestered on the passive continental margins of the Atlantic and on flooded continental interiors (e.g., Arthur et al. 1984, Bralower 1999, Claypool et al. 1977, Jenkyns & Clayton 1997) as Pangea broke apart, export production increased, and organic matter was buried before it could be oxidized. At the same time, sedimentary carbon was both recycled at subduction zones and transferred to orogenic metasediments as the Tethys Sea and Pacific Ocean basins shrank. The circum-Atlantic sediments have not yet been recycled through subduction during the current Wilson Cycle thereby providing long-term storage of large amounts of isotopically light organic carbon. This biologically mediated increase in organic carbon burial may account for as much as half of the long-term increase in $\delta^{13}\text{C}$ values recorded in marine carbonates ($\delta^{13}\text{C}_{\text{carb}}$) (Katz et al. in press) and organic carbon ($\delta^{13}\text{C}_{\text{org}}$) (Hayes et al. 1999) from the Jurassic to the Miocene (Figure 7, see color insert). Increased organic carbon burial contributed to a gradual depletion in CO_2 from the ocean-atmosphere system and a simultaneous increase in the oxidation state of Earth's surface (Katz et al. in press).

The long-term depletion of CO_2 acted as a feedback mechanism that was a key factor that selected β -carboxylation and C_4 photosynthetic pathways in marine and terrestrial photoautotrophs. Diatoms have β -carboxylation pathways (Morris 1980, Reinfelder et al. 2000) and dominate carbon export production in the modern ocean (Smetacek 1999). The rapid radiation of diatoms in the latter half of the Cenozoic enriched the ^{13}C composition of marine organic matter (Figure 7) (Katz et al., in press).

A decrease in diatom cell size over the Cenozoic may also have affected $\delta^{13}\text{C}_{\text{org}}$ values (Figure 7) (Finkel, Katz, Wright, Schofield, & Falkowski submitted). In general, large phytoplankton cells produce high $\delta^{13}\text{C}_{\text{org}}$ because they tend to have low growth rates and low rates of diffusive flux (Laws et al. 1997, Popp et al. 1998, Rau et al. 1997). Early studies suggested that an increase in diatom size through the Cenozoic might have been responsible for the measured increase in $\delta^{13}\text{C}_{\text{org}}$ (Hayes et al. 1999). However, the median diatom cell size appears to have decreased through the Cenozoic (Finkel, Katz, Wright, Schofield, & Falkowski submitted), which contradicts the assertion of Hayes et al. (1999) that a trend toward larger diatoms alone drove the increase in $\delta^{13}\text{C}_{\text{org}}$. Therefore, an increase in diatom abundance (rather than size) since the mid-Cenozoic likely contributed to the $\delta^{13}\text{C}_{\text{org}}$ increase (Finkel, Katz, Wright, Schofield, & Falkowski submitted, Katz et al. in press).

Terrestrial ecosystems also contributed to the $\delta^{13}\text{C}_{\text{org}}$ increase. In the late Miocene (6 to 8 Ma), a global expansion of grasslands was coupled with a shift in dominance from C_3 to C_4 grasses. This shift produced ^{13}C -enriched terrestrial biomass (Cerling et al. 1997, Still et al. 2003), some of which was ultimately transferred to and sequestered in the oceans (France-Lanord & Derry 1994, Hodell 1994) at the same that ^{13}C -enriched diatoms continued to expand. These new pathways are responsible for the $\delta^{13}\text{C}_{\text{org}}$ increase since the mid-Cenozoic, and contributed to the $\delta^{13}\text{C}_{\text{carb}}$ decrease that began in the mid-Miocene (Figure 7). The abrupt $\delta^{13}\text{C}_{\text{org}}$ increase occurred without a large change in either the atmospheric oxidation state or an injection of ^{12}C from mantle outgassing, and appears to be a unique event in Earth's history.

Whereas biological fractionation of carbon isotopes by phytoplankton is a major component of the carbon cycle, fractionation of sulfur isotopes occurs primarily through bacterial reduction of sulfate to sulfide. The carbon and sulfur cycles are linked because bacterial sulfate reduction depends on high levels of sedimentary organic matter. Sulfate reduction can result in pyrite burial, which drives $\delta^{34}\text{S}$ of marine sulfate higher. For atmospheric oxygen levels to remain stable, the carbon and sulfur cycles must be counterbalanced so that as one reduced reservoir grows, the other shrinks (e.g., more organic carbon and less pyrite). In the simplest scenario, this hypothetical relationship indicates that intervals of high $\delta^{13}\text{C}_{\text{carb}}$ should coincide with intervals of low $\delta^{34}\text{S}_{\text{sulfate}}$. In reality, this relationship is complicated by other factors, and redox conditions have fluctuated during times when the two cycles were not counterbalanced, especially on short timescales (e.g., Kump 1993, Payton et al. 1998, Strauss 1999). This situation appears to have been the case not only for some brief intervals, but also for the Jurassic to the Neogene, when the long-term trends in both isotope records show increasing values. These trends indicate that there were increases in the sedimentary reservoirs of reduced carbon (= organic matter) and reduced sulfur (= pyrite), which in turn requires corresponding increases in the oxidized species of both carbon and sulfur. This relationship supports the overall increase in the oxidation state of Earth's surface over this long time period (Katz et al. in press) (Figure 7).

Primary Productivity and Geochemical Proxy Records

Changes in phytoplankton taxonomic composition can influence the carbon isotope record on shorter timescales, as well. Extended intervals of elevated global $\delta^{13}\text{C}_{\text{carb}}$ values are superimposed on the long-term $\delta^{13}\text{C}$ increase from the Jurassic to the mid-Miocene (Figure 7). These intervals typically have been attributed to increases in organic carbon burial relative to carbonate burial that resulted from changes in a combination of surface ocean productivity and/or preservation on the seafloor (e.g., Miller & Fairbanks 1985, Scholle & Arthur 1980, Vincent & Berger 1985). Burial of isotopically light organic carbon leaves the remaining mobile carbon reservoir isotopically heavier, which drives $\delta^{13}\text{C}_{\text{carb}}$ higher. Comparisons among the records of $\delta^{13}\text{C}_{\text{carb}}$, $^{87}\text{Sr}/^{86}\text{Sr}$, and phosphorous flux may provide further insight into these relationships (Figure 7).

Phosphorous is essential for all cells; this element is required for the synthesis of nucleic acids, metabolism of carbohydrates, and formation of membrane lipids. It is supplied only through continental erosion and riverine delivery to the oceans, where it is either used quickly or authigenically precipitated. Phosphorous can be recycled in the upper ocean as organic matter is oxidized and phosphorous is returned to the surface. Because primary production can be limited by phosphorous availability, we compare proxies for productivity ($\delta^{13}\text{C}_{\text{carb}}$) (Katz et al. in press) with phosphorous flux (Follmi 1995) (Figure 7). Episodes of elevated $\delta^{13}\text{C}_{\text{carb}}$ tend to be accompanied by higher phosphorous fluxes prior to the mid-Miocene, although the inverse is not true (this difference may in part reflect the global [$\delta^{13}\text{C}_{\text{carb}}$] versus regional [phosphorous flux] nature of the records). The phosphorous flux and $\delta^{13}\text{C}_{\text{carb}}$ curves decouple most notably during two time intervals: (a) in the Late Cretaceous, when widespread deposition of chalks occurred in shallow waters, where organic carbon must have been oxidized, and (b) in the late Cenozoic, when widespread glaciation increased erosional rates and phosphorous supply to the oceans. These comparisons indicate that phosphorous is not always a limiting nutrient on geological timescales.

Strontium isotopes may provide another clue to link biogeochemical records. In a simple two-source system (Caldeira 1992), strontium is delivered to the oceans through hydrothermal exchange at midocean ridges (low $^{87}\text{Sr}/^{86}\text{Sr}$ values) and continental erosion (high $^{87}\text{Sr}/^{86}\text{Sr}$ values); however, the $^{87}\text{Sr}/^{86}\text{Sr}$ may be complicated by changes in dominant continental source rock type (e.g., Ravizza 1993) and variable riverine fluxes (e.g., Lear et al. 2003). Over the past 200 myr, four out of five decreases in $^{87}\text{Sr}/^{86}\text{Sr}$ values correspond to major episodes of elevated $\delta^{13}\text{C}_{\text{carb}}$ values (Figure 7). The fifth decrease occurs in the Turonian across a data gap in our $\delta^{13}\text{C}_{\text{carb}}$ record, but may correlate to a smaller, shorter interval of elevated $\delta^{13}\text{C}_{\text{carb}}$ documented in published Tethyan records (Jenkyns et al. 1994, Stoll & Schrag 2000). The causal mechanisms behind these correlations are unclear, but may be related to higher pCO_2 from increased hydrothermal activity (e.g., Berner 1993) that accelerated the geological and biological components of the global carbon cycle.

SUMMARY

Cyclic tectonic changes superimposed on key secular changes in Earth's atmosphere, oceans, and even on land have selected for certain phytoplankton clades through time, with an ever-increasing tempo of phytoplankton evolution. In this paper, we have focused on the evolutionary paths that eventually led to the eukaryotic phytoplankton that dominate the contemporary oceans—coccolithophores, diatoms, and dinoflagellates. The earliest primary producers were prokaryotes. For much of the Archaen and Proterozoic Eons, the oceans were dominated by cyanobacteria, with green and perhaps other algae increasing in importance toward the end of the Precambrian. Planktonic algae radiated in the Early Phanerozoic oceans, cyst-forming dinoflagellates and calcareous nannoplankton dominated in the Mesozoic oceans, and, finally, the diatoms rose to prominence in the latter half of the Cenozoic. The primary producers have always been at the base of the food web; hence, the evolution of organisms at higher trophic levels has depended on the evolutionary trajectories of the phytoplankton. The number of invertebrate species relative to phytoplankton species has increased through the Phanerozoic.

This evolutionary succession of marine phytoplankton was a response to a complex system that cannot be explained by a set of ordinary differential equations. Secular shifts in redox seawater chemistry have influenced phytoplankton evolutionary trajectories, both by altering the trace metal availability in the oceans and by changing the balance of fixed nitrogen between the oxidized form (nitrate) and the reduced form (ammonium). In general, the more reducing conditions of the early oceans favored the green lineage, while the higher oxidation states of the later oceans favored the red lineage. Early eukaryotic phytoplankton were best able to compete in the better-oxygenated coastal regions, while green phytoflagellates thrived in open ocean surface waters, where seawater remained Fe rich and relatively Zn and Cd poor (Anbar & Knoll 2002, Whitfield 2001b). Diversity increases in phytoplankton appear to correlate with continental rifting of Rodinia (Late Proterozoic), Pannotia (Early Paleozoic), and Pangea (Jurassic), which ultimately resulted in the three groups of eukaryotic phytoplankton that dominate the modern ocean: coccolithophores, diatoms, and dinoflagellates.

While changing environmental conditions selected for different plankton groups through Earth history, phytoplankton, in turn, influenced biogeochemical components of the environment, often through the biologically mediated oxidation and reduction processes that alter mobile elemental reservoirs. The best example of this process is the role that plankton played in oxygenating Earth's atmosphere and oceans through the evolution of oxygenic photosynthesis. The subsequent rise of the eukaryotic phytoplankton since the Early Jurassic, coupled with the opening of the Atlantic Ocean basin during the current Wilson Cycle, has increased the efficiency of organic carbon burial and contributed to a gradual depletion of CO₂ from the oceans and atmosphere, with a simultaneous increase in the oxidation state of Earth's surface. Ultimately, this change favors the red lineage.

ACKNOWLEDGMENTS

We thank Ken Miller, Oscar Schofield, and Scott Wing for their comments on this manuscript, Ben Cramer for his assistance with statistical analyses, and Richard Bambach for discussions and for providing his revised version of Jack Sepkoski's marine invertebrate database. This study was supported by NSF OCE 00,84032 Biocomplexity: The Evolution and the Radiation of Eukaryotic Phytoplankton Taxa (EREUPT).

**The *Annual Review of Ecology, Evolution, and Systematics* is online at
<http://ecolsys.annualreviews.org>**

LITERATURE CITED

- Alexandre A, Meunier J-D, Colin F, Koud J-M. 1997. Plant impact on the biogeochemical cycle of silicon and related weathering processes. *Geochim. Cosmochim. Acta* 61:677–82
- Alvarez LW, Alvarez W, Asaro F, Michel HV. 1980. Extraterrestrial cause for the Cretaceous-Tertiary extinction. *Science* 208:1095–108
- Anbar AD, Knoll AH. 2002. Proterozoic ocean chemistry and evolution: A bioinorganic bridge? *Science* 297:1137–42
- Arthur M, Sageman B. 1994. Marine black shales: depositional mechanisms and environments of ancient deposits. *Annu. Rev. Earth Planet. Sci.* 22:499–51
- Arthur MA, Dean WE, Stow DAV. 1984. Models for the deposition of Mesozoic-Cenozoic fine-grained organic-C rich sediment in the deep sea. In *Fine-grained Sediments: Deep-water Processes and Facies*, ed. DAV Stow, DJW Piper, pp. 527–59. London: Geological Society of London Special Publication
- Baldauf SL. 2003. The deep roots of eukaryotes. *Science* 300:1703–6
- Baldauf SL, Roger AJ, Wenk-Siefert I, Doolittle WF. 2000. A kingdom-level phylogeny of eukaryotes based on combined protein data. *Science* 290:972–77
- Bambach RK. 1977. Species richness in marine benthic habitats through the Phanerozoic. *Paleobiology* 3:152–67
- Bambach RK. 1993. Seafood through time: changes in biomass, energetics, and productivity in the marine ecosystem. *Paleobiology* 19:372–97
- Bambach RK. 1999. Energetics in the global marine fauna: A connection between terrestrial diversification and change in the marine Biosphere. *Geobios* 32:131–44
- Bambach RK, Knoll AH, Sepkoski JJ. 2002. Anatomical and ecological constraints on Phanerozoic animal diversity in the marine realm. *Proc. Natl. Acad. Sci. USA* 99:6854–59
- Banse K. 1992. Grazing, temporal changes of phytoplankton concentrations, and the microbial loop in the open sea. In *Primary Productivity and Biogeochemical Cycles in the Sea*, ed. PG Falkowski, pp. 409–40. New York: Plenum
- Banse K. 1964. On the vertical distribution of zooplankton in the sea. *Prog. Oceanogr.* 2:53–125
- Barron JA. 2003. Planktonic marine diatom record of the past 18 m.y.: appearances and extinctions in the Pacific and Southern Oceans. *Diatom Res.* 18:203–24
- Bartoli F. 1983. The biogeochemical cycle of silicon in two temperate forest ecosystems. *Ecol. Bull.*:469–76
- Bekker A, Holland HD, Wang P-L, Rumble III D, Stein HJ, et al. 2004. Dating the rise of atmospheric oxygen. *Nature* 427:117–20
- Berggren WA, Kent DV, Swisher CC, Aubry M-P. 1995. A revised Cenozoic geochronology

- and chronostratigraphy. In *Geochronology, Time Scales and Global Stratigraphic Correlations: A Unified Temporal Framework for an Historical Geology*, Special Publ. No. 54, ed. WA Berggren, DV Kent, J Hardenbol, pp. 129–212. Tulsa, OK: SEPM (Society for Sedimentary Geology)
- Berner RA. 1993. Paleozoic atmospheric CO₂: Importance of ocean radiation and plant evolution. *Science* 261:68–70
- Bhattacharya D, Medlin L. 1998. Algal phylogeny and the origin of land plants. *Plant Physiol.* 116:9–15
- Bidle KD, Azam F. 1999. Accelerated dissolution of diatom silica by marine bacterial assemblages. *Nature* 397:508–12
- Bown PR. 1998. *Calcareous Nannofossil Biostratigraphy*. pp. 1–315. London: Kluwer Academic Publishers
- Bown PR, Lees JA, Young JR. 2004. Calcareous nannoplankton diversity and evolution through time. In *Coccolithophores— from Molecular Processes to Global Impact*, ed. H Thierstein, JR Young, pp. 481–507
- Bralower TJ. 1999. The record of global change in mid-Cretaceous (Barremian-Albian) sections from the Sierra Madre, northeast Mexico. *J. Foram. Res.* 29:418–37
- Brasier MD, Green OR, Jephcoat AP, Klepeck AK, Van Kranendonk MJ, et al. 2002. Questioning the evidence for Earth's oldest fossils. *Nature* 416:76–81
- Brocks JJ, Buick R, Summons RE, Logan GA. 2003. A reconstruction of Archean biological diversity based on molecular fossils from the 2.78 to 2.45 billion-year-old Mount Bruce Supergroup, Hamersley Basin, Western Australia. *Geochim. Cosmochim. Acta* 67:4321–35
- Brocks JJ, Logan GA, Buick R, Summons RE. 1999. Archean molecular fossils and the early rise of eukaryotes. *Science* 285:1033–36
- Bujak JP, Williams GL. 1979. Dinoflagellate diversity through time. *Mar. Micropal.* 4:1–12
- Bukry D. 1971. Discoaster evolutionary trends. *Micropaleontology* 17:43–52
- Butterfield NJ. 1997. Plankton ecology and the Proterozoic-Phanerozoic transition. *Paleobiology* 23:247–62
- Butterfield NJ. 2000. *Bangiomorpha pubescens* n. gen., n. sp.: implications for the evolution of sex, multicellularity, and the Mesoproterozoic/Neoproterozoic radiation of eukaryotes. *Paleobiology* 26:386–404
- Butterfield NJ. 2002. *A Vaucheria-like fossil from the Neoproterozoic of Spitsbergen*. Presented at Geol. Soc. Am. Abstracts with Programs, Denver, CO
- Caldeira K. 1992. Enhanced Cenozoic chemical weathering and the subduction of pelagic carbonate. *Nature* 357:578–81
- Canfield DE. 1998. A new model for Proterozoic ocean chemistry. *Nature* 396:450–53
- Cavalier-Smith T. 2003. Genomic reduction and evolution of novel genetic membranes and protein-targeting machinery in eukaryote-eukaryote chimaeras (meta-algae). *Philos. Trans. R. Soc. London Ser. B* 358:109–34
- Cerling TE, Harris JM, MacFadden BJ, Leakey MG, Quade J, et al. 1997. Global vegetation change through the Miocene/Pliocene boundary. *Nature* 389:153–58
- Chacon-Baca E, Beraldi-Campesi H, Cevallos-Ferriz SRS, Knoll AH, Golubic S. 2002. 70 Ma nonmarine diatoms from northern Mexico. *Geology* 30:279–81
- Claypool GE, Lubeck CM, Bayeinger JP, Ging TG. 1977. Organic Geochemistry. In *Geological Studies on the COST No. B-2 Well, U.S. Mid-Atlantic Outer Continental Shelf Area*, ed. PA Scholle, pp. 46–59. Reston, VA: United States Geological Survey
- Colbath GK, Grenfell HR. 1995. Review of biological affinities of Paleozoic acid-resistant, organic-walled eukaryotic algal microfossils (including "acritarchs"). *Rev. Palaeobot. Palynol.* 86:287–314
- Conley DJ. 2002. Terrestrial ecosystems and the global biogeochemical silica cycle. *Glob. Biogeochem. Cycles* 16:1121:doi10.1029/2002GB001894
- Damsté JSS, Muyzer G, Abbas B, Rampen SW, Massé G, et al. 2004. The rise of the Rhizosolenid diatoms. *Science* 304:584–87
- De La Rocha CL, Brzezinski MA, DeNiro MJ.

2000. A first look at the distribution of the stable isotopes of silicon in natural waters. *Geochim. Cosmochim. Acta* 64:2467–77
- Delwiche CF. 1999. Tracing the thread of plastid diversity through the tapestry of life. *Am. Nat.* 154:S164–S77
- Dugdale R, Wilkerson F, Wilkerson. 1998. Silicate regulation of new production in the equatorial Pacific upwelling. *Nature* 391:270–73
- Erbacher J, Thurow J. 1997. Influence of oceanic anoxic events on the evolution of mid-K radiolaria in the North Atlantic and western Tethys. *Mar. Micropaleontol.* 30: 139–58
- Falkowski P, Laws EA, Barber RT, Murray JW. 2003a. Phytoplankton and their role in primary, new and export production. In *Ocean Biogeochemistry. The Role of the Ocean Carbon Cycle in Global Change*, ed. MJR Fasham, pp. 99–121. Berlin: Springer-Verlag
- Falkowski PG, Katz ME, Knoll A, Quigg A, Raven JA, et al. 2004a. The evolution of modern eukaryotic phytoplankton. *Science* 305:354–60
- Falkowski PG, Laws EA, Barber RT, Murray JW. 2003b. Phytoplankton and their role in primary, new, and export production. In *Ocean Biogeochemistry: A JGOFS Synthesis*, ed. MJR Fasham, pp. 99–121. Berlin: Springer-Verlag
- Falkowski PG, Raven JA. 1997. *Aquatic Photosynthesis*. Malden, MA: Blackwell Sci.. 375 pp.
- Falkowski PG, Schofield O, Katz ME, van de Schootbrugge B, Knoll A. 2004b. Why Is the Land Green and the Ocean Red? In *Coccolithophores—from Molecular Processes to Global Impact*, ed. H Thierstein, JR Young, pp. 429–53. Amsterdam: Elsevier
- Fast NM, Kissinger JC, Roos DS, Keeling PJ. 2001. Nuclear-encoded, plastid-targeted genes suggest a single common origin for apicomplexan and dinoflagellates plastids. *Mol. Biol. Evol.* 18:418–26
- Fensome RA, MacRae RA, Moldowan JM, Taylor FJR, Williams GL. 1996. The early Mesozoic radiation of dinoflagellates. *Paleobiology* 22:329–38
- Field C, Behrenfeld M, Randerson J, Falkowski P. 1998. Primary production of the biosphere: integrating terrestrial and oceanic components. *Science* 281:237–40
- Fischer AG, ed. 1984. Catastrophes and Earth History. In *The Two Phanerozoic Supercycles*, ed. WA Berggren, JA van Couvering, pp. 129–50 Princeton, NJ: Princeton Univ. Press
- Follmi KB. 1995. 160 m.y. record of marine sedimentary phosphorus burial: coupling of climate and continental weathering under greenhouse and icehouse conditions. *Geology* 23:859–62
- France-Lanord C, Derry LA. 1994. $\delta^{13}\text{C}$ of organic carbon in the Bengal Fan: source evolution and transport of C_3 and C_4 plant carbon to marine sediments. *Geochim. Cosmochim. Acta* 58:4809–14
- German TN. 1990. *Organic World One Billion Years Ago*. Leningrad: Nauka.
- Gersonde R, Harwood DM. 1990. Lower Cretaceous diatoms from ODP Leg 113 Site 693 (Weddell Sea). Part 1: vegetative cells. In *Proceedings of the Ocean Drilling Program, Scientific Results*, ed. PF Barker, JP Kennett, SB O’Connell, pp. 365–402. College Station, TX: Ocean Drilling Program
- Ghil M, Allen MR, Dettinger MD, Ide K, Kondrashov D, et al. 2002. Advanced spectral methods for climatic time series. *Rev. Geophys.* 40:10.1029/2000RG000092
- Gradstein FM, Agterberg FP, Ogg JG, Hardenbol H, van Veen P, et al. 1995. A Triassic, Jurassic, and Cretaceous time scale. In *Geochronology, Time Scales and Global Stratigraphic Correlations: A Unified Temporal Framework for an Historical Geology*, Special Publ. No. 54, ed. WA Berggren, DV Kent, J Hardenbol, pp. 95–126. Tulsa, OK: SEPM (Society for Sedimentary Geology)
- Grantham PJ, Wakefield LL. 1988. Variations in the sterane carbon number distributions of marine source rock derived crude oils through geological time. *Org. Geochem.* 12: 61–73
- Gray MW, Lang BF, Cedergreen R, Golding

- GB, Lemieux C, et al. 1998. Genome structure and gene content in protist mitochondrial DNAs. *Nucleic Acids Res.* 26:865–78
- Grover JP. 1988. Dynamics of competition in a variable environment: experiments with two diatom species. *Ecology* 69:408–17
- Grover JP. 1991. Resource competition in a variable environment: phytoplankton growing according to the variable-internal-stores model. *Am. Nat.* 138:811–35
- Grzebyk D, Schofield O, Vetriani C, Falkowski PG. 2003. The Mesozoic radiation of eukaryotic algae: The portable plastid hypothesis. *J. Phycol.* 39:259–67
- Hamm CE, Merkel R, Springer O, Jurkojc P, Maier C, et al. 2003. Architecture and material properties of diatom shells provide effective mechanical protection. *Nature* 421:841–43
- Han TM, Runnegar B. 1992. Megascopic eukaryotic algae from the 2.1-billion-year-old Negaunee iron-formation, Michigan. *Science* 257:232–35
- Haq BU, Hardenbol J, Vail PR. 1987. Chronology of fluctuating sea levels since the Triassic (250 million years ago to present). *Science* 235:1156–67
- Hardie LA. 1996. Secular variation in seawater chemistry: an explanation for the coupled secular variation in the mineralogies of marine limestones and potash evaporites over the past 600 m.y. *Geology* 24:279–83
- Harper JT, Keeling PJ. 2003. Nucleus-encoded, plastid-targeted glyceraldehyde-3-phosphate dehydrogenase (GAPDH) indicates a single origin for chromalveolate plastids. *Mol. Biol. Evol.* 20:1730–35
- Harwood DM, Gersonde R. 1990. Lower Cretaceous diatoms from ODP Leg 113 Site 693 (Weddell Sea). Part 2: Resting spores, Chrysophycean cysts, and endoskeletal dinoflagellate, and notes on the origin of diatoms. In *Proc. Ocean Drilling Program*, ed. PF Barber, JP Kennett, et al., 403–25. College Station, TX: Ocean Drilling Program
- Harwood DM, Nikolaev VA. 1995. Cretaceous diatoms: morphology, taxonomy, biostratigraphy. In *Siliceous Microfossils*, ed. CD Blome, PM Whalen, R Katherine, pp. 81–106. Lawrence, KS: Paleontological Society
- Hayes JM, Strauss H, Kaufman AJ. 1999. The abundance of ^{13}C in marine organic matter and isotopic fractionation in the global biogeochemical cycle of carbon during the past 800 Ma. *Chem. Geol.* 161:103–25
- Hess WR, Rocap G, Ting CS, Larimer F, Stilwagen S, et al. 2001. The photosynthetic apparatus of *Prochlorococcus*: Insights through comparative genomics. *Photosynth. Res.* 70:53–71
- Hodell DA. 1994. Magnetostratigraphic, biostratigraphic, and stable isotope stratigraphy of an Upper Miocene drill core from the Sale Briqueterie (northwestern Morocco): a high-resolution chronology for the Messinian stage. *Paleoceanography* 9:835–55
- Houghton SD. 1991. Calcareous nannofossils. In *Calcareous Algae and Stromatolites*, ed. R Riding, pp. 217–66. Berlin: Springer-Verlag
- Howarth RJ, McArthur JM. 1997. Statistics for strontium isotope stratigraphy: A robust LOWESS fit to the marine Sr-isotope curve for 0 to 206 Ma, with look-up table for derivation of numeric age. *J. Geol.* 105:441–56
- Isozaki Y. 1997. Permo-Triassic boundary superanoxia and stratified superocean: records from lost deep sea. *Science* 276:235–38
- Jacobs BF, Kingston JD, Jacobs LL. 1999. The origin of grass-dominated ecosystems. *Ann. Mo. Bot. Gard.* 86:590–643
- Janis CM, Damuth J, 2000. Mammals. In *Evolutionary Trends*, ed. KJ McNamara, pp. 301–45. London: J. Belknap.
- Janofske D. 1992. Calcareous Nannofossils of the Alpine Upper Triassic, In *Nannoplankton Research*, ed. B Hamrsmid, JR Young, 1:87–109. Knihovnicka ZPZ.
- Javaux EJ, Knoll AH, Walter MR. 2001. Morphological and ecological complexity in early eukaryotic ecosystems. *Nature* 412:66–69
- Jeffrey SW, Mantoura RFC, Wright SW. 1997. *Phytoplankton Pigments in Oceanography: Guidelines to Modern Methods*. Paris: UNESCO Publishing. 661 pp.

- Jenkyns HC, Clayton CJ. 1997. Lower Jurassic epicontinental carbonates and mudstones from England and Wales: chemostratigraphic signals and the early Toarcian anoxic event. *Sedimentology* 44:687–706
- Jenkyns HC, Gale AS, Corfield RM. 1994. Carbon- & oxygen-isotope stratigraphy of the English chalk & Italian Scaglia & its palaeoclimatic significance. *Geol. Mag.* 131:1–34
- Kamykowski D. 1981. Laboratory experiments on the diurnal verticle migration of marine dinoflagellates through temperature gradient. *Mar. Biol.* 62:57–64
- Katz ME, Wright JD, Miller KG, Cramer BS, Fennel K, Falkowski PG. 2004. Biological overprint of the geological carbon cycle. *Marine Geol.* In press
- Kellogg EA. 2000. The grasses: a case study in macroevolution. *Ann. Rev. Ecol. Syst.* 31: 217–38
- Knoll AH. 1989. Evolution and extinction in the marine realm: some constraints imposed by phytoplankton. *Phil. Trans. R. Soc. London Ser. B* 325:279–90
- Knoll AH. 1992. The early evolution of eukaryotes: A geological perspective. *Science* 256:622–27
- Knoll AH. 1994. Proterozoic and Early Cambrian protists: evidence for accelerating evolutionary tempo. *Proc. Natl. Acad. Sci. USA* 91:6743–50
- Knoll AH. 2003. *Life on a Young Planet: The First Three Billion Years of Evolution on Earth*. Princeton, NJ: Princeton Univ. Press, 277 pp.
- Kump LR, ed. 1993. *The Coupling of the Carbon and Sulfur Biogeochemical Cycles Over Phanerozoic Time, Vol. 14*. Berlin: Springer-Verlag
- Laws EA, Bidigare R, Popp BN. 1997. Effect of growth rate and CO₂ concentration on carbon isotopic fractionation by the marine diatom *Phaeodactylum tricornutum*. *Limnol. Oceanogr.* 42:1552–60
- Lear CH, Elderfield H, Wilson PA. 2003. A Cenozoic seawater Sr/Ca record from benthic foraminiferal calcite and its application in determining global weathering fluxes. *Earth Planet Sci. Lett.* 208:69–84
- Leckie RM, Bralower TJ, Cashman R. 2002. Oceanic anoxic events and plankton evolution: Biotic response to tectonic forcing during the mid-Cretaceous. *Paleoceanography* 17:1–29
- Li WKW. 2002. Macroecological patterns of phytoplankton in the northwestern North Atlantic Ocean. *Nature* 419:154–57
- Lipps JH, ed. 1993. *Fossil Prokaryotes and Protists*. Oxford: Blackwell. 342 pp.
- MacArthur RH, Wilson EO. 1967. *The Theory of Island Biogeography*. 203 pp. Princeton, NJ: Princeton University
- Maldonado M, Carmona MC, Uriz MJ, Cruzado A. 1999. Decline in Mesozoic reef-building sponges explained by silicon limitation. *Nature* 401:785–88
- Margalef R. 1994. Dynamic aspects of diversity. *J. Veg. Sci.* 5:451–56
- McFadden GI. 1999. Plastids and protein targeting. *J. Eukaryot. Microbiol.* 46:339–46
- Medlin LK, Kooistra WCHF, Schmid A-MM. 2000. A review of the evolution of the diatoms—a total approach using molecules, morphology and geology. In *The Origin and Early Evolution of the Diatoms: Fossil, Molecular and Biogeographical Approaches*, ed. A Witkowski, J Sieminska, pp. 13–35. Krakow: Polish Acad. Sci.
- Medlin LK, Kooistra WCHF, Potter D, Saunders GW, Andersen RA. 1997. Phylogenetic relationships of the ‘golden algae’ (haptophytes, heterokont chromophytes) and their plastids. *Plant Syst. Evol.* 11(Suppl.):187–219
- Melkonian M, Surek B. 1995. Phylogeny of the Chlorophyta: Congruence between ultrastructural and molecular evidence. *Bull. Soc. Zool. Fr.* 120:191–208
- Miller KG, Fairbanks RG. 1985. Oligocene to Miocene carbon isotope cycles and abyssal circulation changes. In *The Carbon Cycle and Atmospheric CO₂: Natural Variations Archean to Present*, ed. ET Sundquist, WS Broecker, pp. 469–86. Washington, DC: American Geophysical Union

- Moldowan JM, Dahl J, Jacobson SR, Huizinga BJ, Fago FJ, et al. 1996. Chemostratigraphic reconstruction of biofacies: molecular evidence linking cyst-forming dinoflagellates with pre-Triassic ancestors. *Geology* 24:159–62
- Moldowan JM, Jacobson SR. 2000. Chemical signals for early evolution of major taxa: biosignatures and taxon-specific biomarkers. *Int. Geol. Rev.* 42:805–12
- Moldowan JM, Talyzina NM. 1998. Biogeochemical evidence for dinoflagellate ancestors in the Early Cambrian. *Science* 281:1168–70
- Molyneux SG, Le Hérisse A, Wicander R. 1996. Paleozoic phytoplankton. In *Palynology: Principles and Applications*, ed. J Janzonius, DC McGregor, pp. 493–530. Amer. Assoc. Strat. Palynol. Found.
- Morris I. 1980. Paths of carbon assimilation in marine phytoplankton. In *Primary Productivity in the Sea*, ed. PG Falkowski, pp. 139–59. New York: Plenum
- Müller KM, Oliveira MC, Sheath RG, Bhattacharya D. 2001. Ribosomal DNA phylogeny of the Bangiophycidae (Rhodophyta) and the origin of secondary plastids. *Am. J. Bot.* 88:1390–400
- Oliveira MC, Bhattacharya D. 2000. Phylogeny of the Bangiophycidae (Rhodophyta) and the secondary endosymbiotic origin of algal plastids. *Am. J. Bot.* 87:482–92
- Osyczka A, Moser CC, Daldal F, Dutton PL. 2004. Reversible redox energy coupling in electron transfer chains. *Nature* 427:607–12
- Paerl HW, Valdes LM, Pinckney JL, Piehler MF, Dyble J, Moisaner PH. 2003. Phytoplankton photopigments as indicators of estuarine and coastal eutrophication. *BioScience* 53:953–64
- Palmer JD. 2003. The symbiotic birth and spread of plastids: How many times and who dunit? *J. Phycol.* 39:4–11
- Payton A, Kastner M, Campbell D, Thiemens MH. 1998. Sulfur isotopic composition of Cenozoic seawater sulfate. *Science* 282:1459–62
- Payton A, Kastner M, Campbell D, Thiemens MH. 2004. Seawater sulfur isotope fluctuations in the Cretaceous. *Science* 304:1663–65
- Popp BN, Kenig F, Wakeham SG, Laws EA, Bidigare RR. 1998. Does growth rate affect ketone unsaturation and intracellular carbon isotopic variability in *Emiliania huxleyi*? *Paleoceanography* 13:35–41
- Prauss M. 2000. The oceanographic and climatic interpretation of marine palynomorph phytoplankton distribution from Mesozoic, Cenozoic and Recent sections. *Habilitationsschrift, Gött. Arb. Geol. Paläontol.* 76:1–235
- Quigg A, Finkel ZV, Irwin AJ, Rosenthal Y, Ho T-Y, et al. 2003. Plastid inheritance of elemental stoichiometry in phytoplankton and its imprint on the geological record. *Nature* 425:291–94
- Rapp GJ, Mulholland SC. 1992. *Phytolith Systematics: Emerging Issues*. New York: Plenum
- Rau GH, Riebesell U, Wolf-Gladrow DA. 1997. *Global Biogeochem. Cycles* 11:267
- Raven JA. 1997. The vacuole: A cost-benefit analysis. *Adv. Bot. Res. Adv. Plant Pathol.* 25:59–86
- Ravizza G. 1993. Variations of the 187Os/186Os ratio of seawater over the past 28 million years as inferred from metalliferous carbonates. *Earth Planet. Sci. Lett.* 118:335–48
- Reinfelder JR, Kraepiel AML, Morel FMM. 2000. Unicellular C₄ photosynthesis in a marine diatom. *Nature* 407:996–99
- Retallack GJ. 1997. Cenozoic expansion of grasslands and climatic cooling. *J. Geol.* 109:407–26
- Retallack GJ. 2001. Neogene expansion of the North American prairie. *Palaios* 12:380–90
- Rich JE, Johnson GL, Jones JE, Campsie J. 1986. A significant correlation between fluctuations in seafloor spreading rates and evolutionary pulsations. *Paleoceanography* 1:85–95
- Ronov AB. 1994. Phanerozoic transgressions and regressions on the continents: a quantitative approach based on areas flooded by the sea and areas of marine and continental deposition. *Am. J. Sci.* 294:777–801

- Rosenzweig ML. 1995. *Species Diversity in Space and Time*. Cambridge: Cambridge Univ. Press
- Rosing MT. 1999. C-13-depleted carbon microparticles in >3700-Ma sea-floor sedimentary rocks from west Greenland. *Science* 283:674–76
- Roth PH. 1987. Mesozoic calcareous nannofossil evolution: relation to paleoceanographic events. *Paleoceanography* 2:601–11
- Rothpletz A. 1896. Über die Flysch-Fucoiden und einzige andere fossile Algen, sowie über Liasische Diatomeen führende Hornschwämme. *Deutsch. geol. Ges* 48:858–914
- Sandberg PA. 1975. New interpretations of Great Salt Lake ooids and of ancient nonskeletal carbonate mineralogy. *Sedimentology* 22:497–538
- Scholle PA, Arthur MA. 1980. Carbon isotope fluctuations in Cretaceous pelagic limestones: potential stratigraphic and petroleum explorations tool. *Bull. Am. Assoc. Petroleum Geologists*: 64:67–87
- Schopf JW. 1993. Microfossils of the Early Archean Apex chert: New evidence of the antiquity of life. *Science* 260:640–46
- Schopf JW. 2002. *Life's Origin, The Beginnings of Biological Organization*: Univ. Calif. Press. 208 pp.
- Sepkowski J. 1997. Biodiversity: past, present, and future. *J. Paleont.* 71:533–39
- Shen Y, Canfield DE, Knoll AH. 2002. The chemistry of mid-Proterozoic oceans: evidence from the McArthur Basin, northern Australia. *Am. J. Sci.* 302:81–109
- Shen Y, Knoll AH, Walter MR. 2003. Evidence for low sulphate and anoxia in a mid-Proterozoic marine basin. *Nature* 423:632–35
- Sibley DF, Vogel TA. 1976. Chemical Mass Balance of the Earth's crust: the calcium dilemma (?) and the role of Pelagic sediments. *Science* 551–53
- Siegel DA. 1998. Resource competition in a discrete environment: Why are plankton distributions paradoxical? *Limnol. Oceanogr.* 43: 1133–46
- Smetacek V. 1999. Diatoms and the ocean carbon cycle. *Protist* 150:25–32
- Smetacek V. 2001. A watery arms race. *Nature* 411:745
- Southam JR, Hay WW. 1981. Global sedimentary mass balance and sea level changes. In *The Sea*, ed. C Emiliani, pp. 1617–84. New York: Wiley-Interscience
- Spencer-Cervato C. 1999. The Cenozoic deep sea microfossil record: explorations of the DSDP/ODP sample set using the Neptune database. *Palaeontologia Electronica* 2:1–270
- Stanley GD Jr., Hardie LA. 1998. Secular oscillations in the carbonate mineralogy of reef-building and sediment-producing organisms driven by tectonically forced shifts in seawater chemistry. *Palaeogeogr. Palaeoclimatol. Palaeoecol.* 144:3–19
- Still CJ, Berry JA, Collatz GJ, DeFries RS. 2003. Global distribution of C₃ and C₄ vegetation: carbon cycle implications. *Glob. Biogeochem. Cycles* 17:doi:1029/2001GB001807
- Stoll HM, Schrag DP. 2000. Coccolith Sr/Ca as a new indicator of coccolithophorid calcification and growth rate. *Geochem. Geophys. Geosystems* 1:<http://146.201.54.53/publicationsfinal/articles/1999GC000015/fs1999GC.html>
- Stover LE, Brinkhuis H, Damassa SP, de Verteuil L, Helby RJ, et al. 1996. Mesozoic-Tertiary dinoflagellates, acritarchs & prasinophytes. In *Palynology: Principles and Applications*, ed. J Jansonius, DC McGregor, pp. 641–750: Amer. Assoc. Strat. Palynol Found.
- Strauss H. 1999. Geological evolution from isotope proxy signals—sulfur. *Chem. Geol.* 161:89–101
- Strelnikova NI. 1991. Evolution of diatoms during the Cretaceous and Paleogene periods. Presented at the 10th Diatom Symposium, 1988, Joensuu, Finland
- Summons R, Jahnke L, Hope J, Logan G. 1999. 2-Methylhopanoids as biomarkers for cyanobacterial oxygenic photosynthesis. *Nature* 400:55–57

- Summons RE, Thomas J, Maxwell JR, Boreham CJ. 1992. Secular and environmental constraints on the occurrence of dinosterane in sediments. *Geochim. Cosmochim. Acta* 56: 2437–44
- Summons RE, Walter MR. 1990. Molecular fossils and microfossils of prokaryotes and protists from Proterozoic sediments. *Am. J. Sci.* 290-A: 212–44
- Talyzina NM, Moczydlowska M. 2000. Morphological and ultrastructural studies of some acritarchs from the Lower Cambrian Lukati Formation, Estonia. *Rev. Palaeobot. Palynol.* 112:1–21
- Tappan H. 1980. *The Palaeobiology of Plant Protists*. San Francisco: WH Freeman, 1028 pp.
- Taylor FJR. 1987. An overview of the status of evolutionary cell symbiosis theories. *Ann. NY Acad. Sci.* 503:1–16
- Tilman D. 1977. Resource competition between planktonic algae: an experimental and theoretical approach. *Ecology* 58:338–48
- Tomitani A, Okada K, Miyashita H, Matthijs HCP, Ohno T, Tanaka A. 1999. Chlorophyll *b* and phycobilins in the common ancestor of cyanobacteria and chloroplasts. *Nature* 400:159–62
- Tozzi S, Schofield O, Falkowski PG. 2004. Historical climate change and ocean turbulence as selective agents for two key phytoplankton functional groups. *Mar. Ecol. Prog. Ser.* 274:123–32
- Tréguer P, Nelson DM, van Bennekom AJ, Demaster DJ, Leynaert A, Quéguiner B. 1995. The silica balance in the world ocean: a reestimate. *Science* 268:375–79
- Twitchett R. 1999. Palaeoenvironments and faunal recovery after the end-Permian mass extinction. *Palaeogeogr. Palaeoclimatol. Palaeoecol.* 154:27–37
- Vail PR, Mitchum RM, Thompson III S, eds. 1977. Seismic stratigraphy and global changes of sea level, part 4: Global cycles of relative changes of sea level. In *Seismic Stratigraphy and Global Changes of Sea Level*, Vol. 26, ed. CE Payton, pp. 83–97. Tulsa, OK: American Association of Petroleum Geologists Memoirs
- Valentine JW, Moores EM. 1974. Plate tectonics and the history of life in the oceans. *Sci. Am.* 230:80–89
- Van den Hoek C, Mann DG, Jahns HM. 1995. *Algae: An Introduction to Phycology*. Cambridge: Cambridge Univ. Press. 627 pp.
- Villareal TA, Altabet MA, Culver-Rymsza K. 1993. Nitrogen transport by vertically migrating diatoms mats in the North Pacific Ocean. *Nature* 363:709–12
- Vincent E, Berger WH. 1985. Carbon dioxide and polar cooling in the Miocene: The Monterey Hypothesis. In *The Carbon Cycle and Atmospheric CO₂: Natural Variations Archean to Present*, ed. ET Sundquist, WS Broecker, pp. 455–68. Washington, DC: American Geophysical Union
- Whitfield M. 2001. Interactions between phytoplankton and trace metals in the ocean. *Adv. Mar. Biol.* 41:3–128
- Wignall P, Twitchett R. 2002. Permian-Triassic sedimentology of Jameson Land, East Greenland: incised submarine channels in an anoxic basin. *J. Geol. Soc. London* 159:691–703
- Wilkinson BH, Algeo TJ. 1989. Sedimentary carbonate record of calcium-magnesium cycling. *Am. J. Sci.* 289:1158–94
- Wilson JT. 1966. Did the Atlantic close and then re-open? *Nature* 211:676–81
- Worsley TR, Nance RD, Moody JB. 1986. Tectonic cycles and the history of the Earth's biogeochemical and paleoceanographic record. *Paleoceanography* 1:233–63
- Xiao S, Knoll AH, Yuan X, Pueschel C. 2004. Phosphatized multicellular algae in the Neoproterozoic Doushantuo Formation, China, and the early evolution of florideophyte red algae. *Am. J. Bot.* 91:214–27
- Yoon HS, Hackett JD, Bhattacharya D. 2002a. A single origin of the peridinin- and fucoxanthin-containing plastids in dinoflagellates through tertiary endosymbiosis. *Proc. Natl. Acad. Sci. USA* 99:11724–29

- Yoon HS, Hackett JD, Pinto G, Bhattacharya D. 2002b. The single, ancient origin of chromist plastids. *Proc. Natl. Acad. Sci. USA* 99:15507–12
- Yoon HS, Hackett JD, Ciniglia C, Pinto G, Bhattacharya D. 2004. A Molecular Timeline for the Origin of Photosynthetic Eukaryotes. *Mol. Biol. Evol* 21:809–18
- Zhang Z. 1986. Clastic facies microfossils from the Chuanlingguo Formation near Jixian, north China. *J. Micropaleontol.* 5:9–16

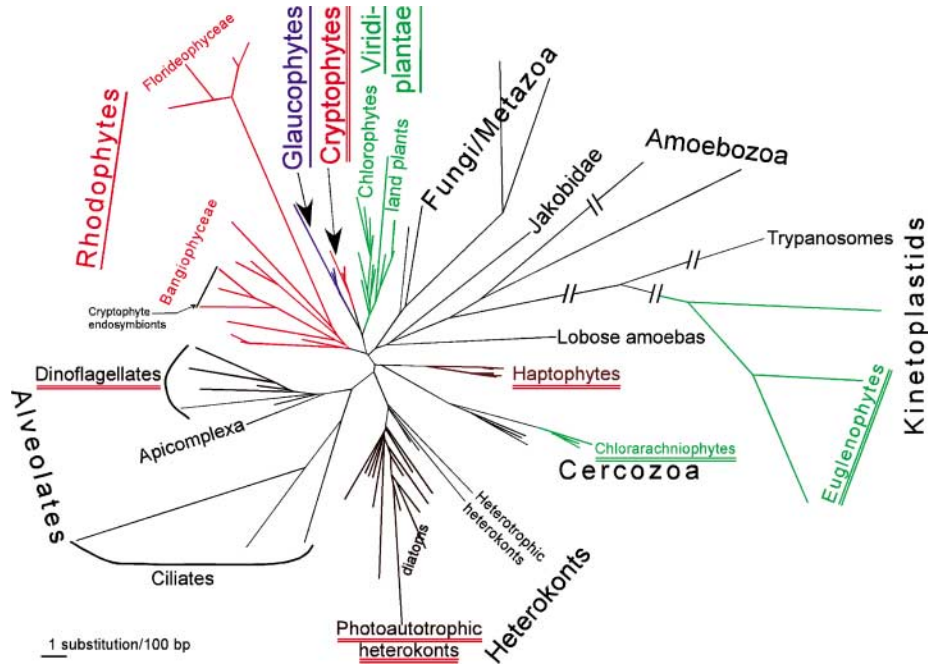


Figure 1 Relationships among photosynthetic eukaryotes inferred from 18S rRNA gene sequences (species names and sequence accession numbers are not shown for the clarity of the figure). Names underlined with one or two strokes indicate taxa that contain primary or secondary endosymbiotic plastids (green or red), respectively. Colored branches indicate taxa that contain photosynthetic plastids. Phylogenetic tree was constructed with the PHYLIP software package, in which genetic distance calculation (F84 substitution model) and the neighbor-joining method were used. Tree displayed is consistent with consensus trees obtained from 1,000 bootstrapped data sets.

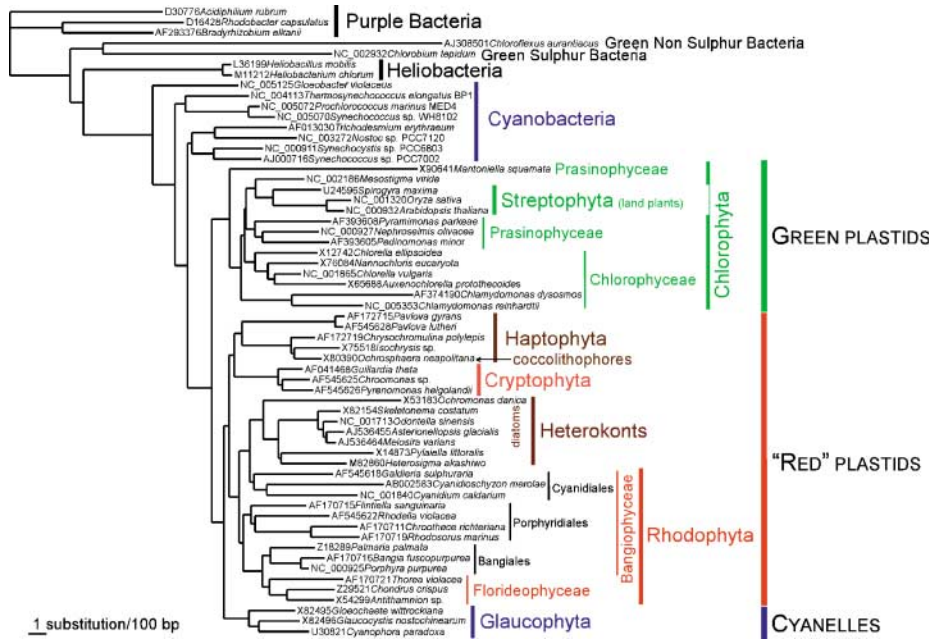
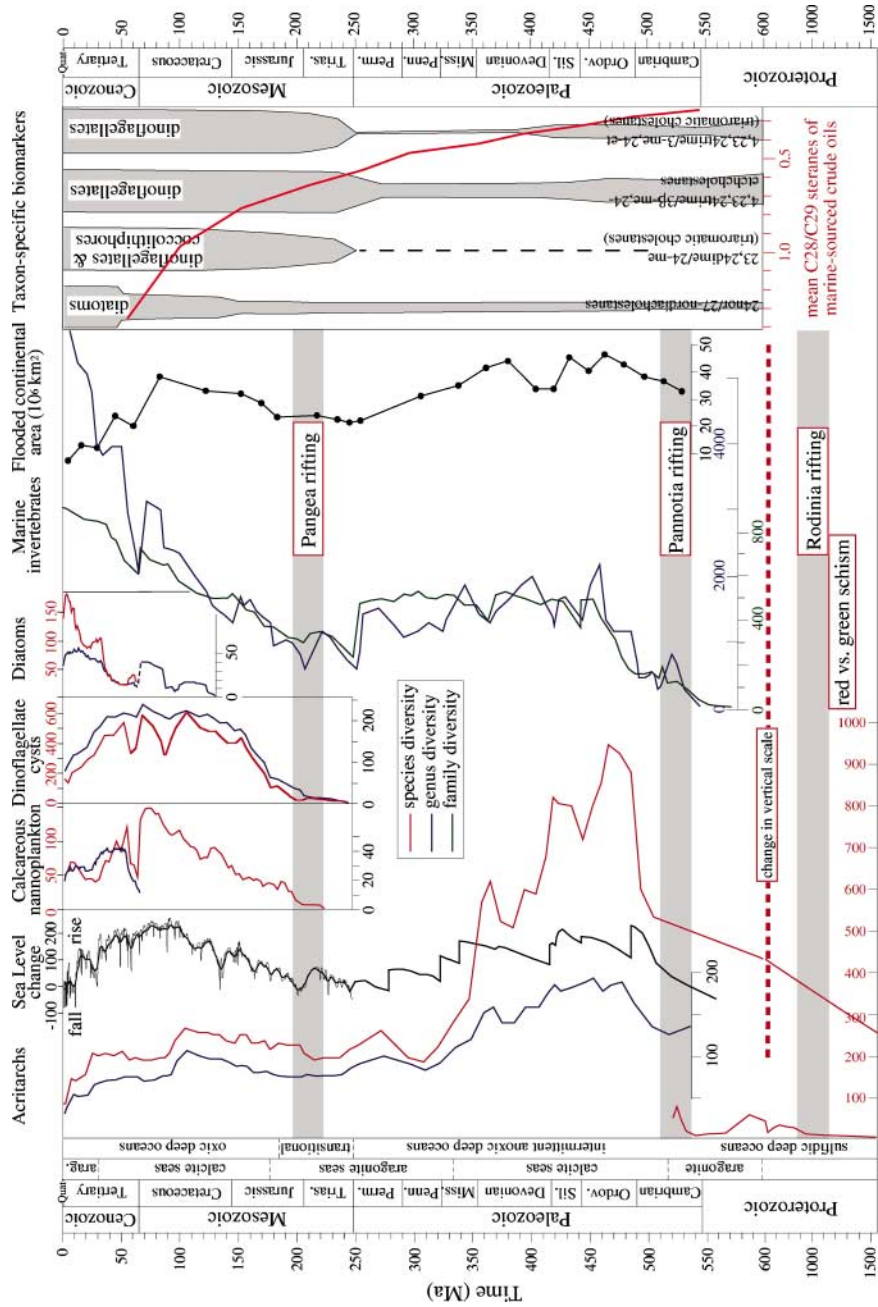


Figure 2 Phylogenetic tree of plastids inferred from 16S rRNA gene sequences rooted with anoxygenic photosynthetic bacteria. Tree shows all plastids originating once from cyanobacteria, likely from an ancestral lineage that subsequently became extinct. Data from euglenophytes and chlororachniophytes (secondary green plastids) and from dinoflagellates (two types of secondary red plastids) have been excluded because of high genetic divergences responsible for inconsistent phylogenetic branchings. Phylogenetic tree was constructed with the PHYLIP software package, in which genetic distance calculation (F84 substitution model) and the neighbor-joining method were used. Tree displayed is consistent with consensus tree obtained from 1,000 bootstrapped datasets. Each species name is preceded by the accession number of the DNA sequence used in the phylogenetic analysis. Colors indicate groups of photosynthetic plastids.

EVOLUTION OF EUKARYOTIC PHYTOPLANKTON C-3



See legend on next page

Figure 3 Comparison of eukaryotic phytoplankton diversity curves (after Katz et al. in press) with sea-level change (Mesozoic-Cenozoic [Haq et al. 1987] and Paleozoic [Vail et al. 1977]), flooded continental areas (Ronov 1994), and marine genus (blue) and family (green) invertebrate diversities (Sepkowski 1997). Phytoplankton species (red) diversities are from published studies (calcareous nanofossils [Bown et al. 2004], dinoflagellates [Stover et al. 1996], diatoms [Spencer-Cervato 1999], acritarchs [Proterozoic {Knoll 1994}], [Phanerozoic {R.A. MacRae, unpublished data}]). Phytoplankton genus (blue) diversities were compiled for this study from publicly available databases (calcareous nanofossils and diatoms [Spencer-Cervato 1999], dinoflagellates, and acritarchs [R.A. MacRae, unpublished data]). All records are adjusted to the Berggren et al. (1995) (Cenozoic), Gradstein et al. (1995) (Mesozoic), and GSA (<http://rock.geosociety.org/science/timescale/timescl.htm>) (Paleozoic) timescales. Taxon-specific biomarkers (Moldowan & Jacobson 2000) and C28/C29 sterane ratios (Grantham & Wakefield 1988) provide a record of increased biomass preservation of eukaryotic phytoplankton in the Mesozoic-Cenozoic. Episodes of supercontinent rifting are shaded. We base our interpretations of acritarch evolution on two compilations: a high-quality Proterozoic and Early Cambrian record of acritarch species (Knoll 1994) and a global, genera-level, Phanerozoic, quality-controlled literature compilation that may include taxonomic synonyms (R.A. MacRae, personal communication). Biological uncertainty exists in the interpretation of different genera and species within the acritarch record. Even though Knoll's (1994) record underestimates global diversity, and MacRae's record overestimates it, the long-term patterns of diversification and extinction appear consistent and robust.

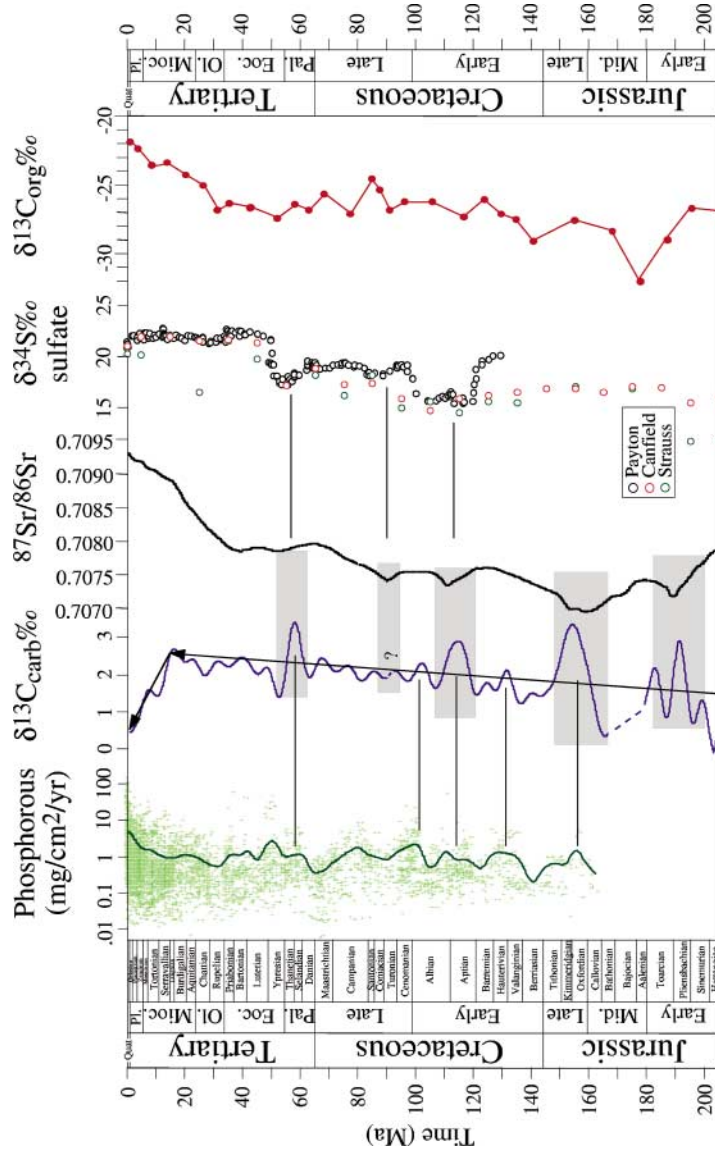


Figure 7 Geochemical proxy records showing comparisons of phosphorous flux [(Follmi 1995); curve fit (B.S. Cramer, personal communication) uses the SSA-MTM Toolkit from <http://www.atmos.ucla.edu/tcd/ssa/> (Ghil et al. 2002)], bulk sediment $\delta^{13}\text{C}_{\text{carb}}$ (Katz et al., in press), strontium isotopes (Howarth & McArthur 1997), sulfur isotopes (Canfield 1998, Payton et al. 1998, Payton et al., 2004, Strauss 1999), and bulk sediment $\delta^{13}\text{C}_{\text{org}}$ (Hayes et al. 1999). Timescales are as in Figure 3.